This is to certify that the

thesis entitled

A Finite Element Analysis of Plated Bones

presented by

Michael H. Schwartz

has been accepted towards fulfillment
of the requirements for

Master of Science degree in Mechanics

Major professor

Date 5/18/88

A FINITE ELEMENT ANALYSIS OF PLATED BONES

By

Michael Hart Schwartz

A THESIS

Submitted to
Michigan State University
in partial fulfillment of the requirements
for the degree of

MASTER OF SCIENCE

Department of Metallurgy, Mechanics and
Materials Science

1988

ABSTRACT

A FINITE ELEMENT ANALYSIS OF PLATED BONES

By

Michael Hart Schwartz

In an effort to study the mechanics of plated bones, a finite element model was created and verified through a process of mesh refinement. A series of load cases and material property modifications were analyzed in order to demonstrate the model's capabilities. Increasing plate stiffness resulted in shunting of stress away from the bone and into the plate. It was found that the load bearing role of the fasteners reversed under a reversal of applied load. Finally, it was found that for plates with a small Young's modulus, the bone underwent a rotation about its axis due to fastener pattern asymmetry. Results are displayed in the form of line graphs and stress plots, and recommendations for future modelling considerations are made.

This thesis is dedicated to:

My parents for their love and support.

Joia, for her love, friendship and compassion

All of my friends and roommates for putting up with me

Andy Hull for his help with ANSYS, etc...

Dave Miner, for his help with Al and Sarah.

and,

Dr. Robert William Soutas-Little for supporting me since I was an undergraduate, and advising me in my research.

ACKNOWLEDGMENTS

I would like to acknowledge United States Surgical Corporation for their financial support of this research.

TABLE OF CONTENTS

LIST OF TABLES

LIST OF FIGURES

LIST OF SYMBOLS

A	Cross sectional area
a_n, b_n	Fourier coefficients
C	Damping coefficient of gap element
C3,C4	Constants of integration
d	Distance to centroid
E	Young's Modulus
e(x)	Truncation error
Fs_i	Force in spring number i in beam model
I	Moment of inertia
K_i	Stiffness of spring number i in beam model
K2	Stiffness of gap element
l_p	Length of plate
l_b	Length of bone
l_i	Length to spring number i in beam model
M_p	Moment in plate
M_b	Moment in bone
M_A	Applied moment
N	Number of springs in beam model
N	Truncation point for Fourier series
Pa	Pascals (N/m^2)
R	Reaction force due to contact
v_b	Deflection of bone

v_p	Deflection of plate
v_p'	Slope of plate
v_o	Downward displacement of bone at osteotomy
ϕ	Angle of out of plane rotation
ϕ, ψ	Incompatible shear angles
σ	Cauchy stress
θ	Slope of bone at osteotomy
θ	Shear angle
$< \quad >^i$	Singularity function of order i

I. INTRODUCTION

Long bones are the elements of the skeletal system designed to supply the majority of the support for the body. They consist of two architecturally distinct parts, a hollow shaft (diaphysis) comprised of compact bone, and two ends (epiphyses) consisting of a spongy (cancellous) bone interior covered with a thin layer of compact bone. It is the compact bone in the diaphysis which is responsible for the strength of the entire bone; therefore, the integrity of the diaphysis is imperitive for normal function.

Occasionaly, whether through accident, or surgical procedure, a diaphyseal fracture may occur. In this event, the objectives for treatment are twofold. First and foremost, active function of the joints of the part must take place. Secondly, the sight of the fracture and its surrounding areas must heal in a manner so that their original strength is returned. Unfortunately, these two goals tend to be counteractive. In general, the immobilization required for union to occur causes osteopenias of the bone characterized by a thinning of the cortical layer and an increase in the diameter of the haversian canals.

In order to facilitate both of the goals of healing, the use of internal bone plating was developed and advanced in the early and mid 1940's (Horowitz,Key,Murray)[13,14,19]. By securing a plate across the osteotomy, the sight is fixed thus allowing the bone to withstand the stresses and strains associated with re-mobilization of the limb while still maintaining close proximity of the fragments at the osteotomy.

Internal bone plates do not, however, provide a complete solution to the problem. If the plate is too rigid, stress is shunted away from the bone, through the plate, and the tissues around the osteotomy atrophy and become weak. If the plate is too flexible, motion occurs at the osteotomy and poor reduction of the fracture follows, again resulting in a weak structure. Bones fixed by flexible plates have the additional problem that they run a high risk of failure by means of plate fracture or fastener pullout.

In order to investigate these phenonena, analytical models have been developed which can yield the stress and displacement fields of the plate and bone, thus allowing conclusions to be drawn about the effectiveness of different designs without the need for costly and time consuming experiments. While early researchers employed composite beam theory for this end, advances in digital computers and new software resulted in the widespread use of the finite element method as a means for accurately predicting the mechanical response of plated fractures.

The following paper describes research to develop a finite element model of a plated long bone. A verification process will be documented for each model, from the one dimensional strength of materials solution to the final finite element mesh. Finally, the results obtained from a series of load configurations and variations of material properties will be displayed and the pertinence to possible design or operative modifications as well as Wolff's law will be discussed.

II. SURVEY OF LITERATURE

In 1892, Julius Wolff[36] proposed a set of hypotheses based on experimental observation which stated that the architecture of bone is determined in some way by the stress field to which it is subjected. Since that time, a great deal of effort has been put forth by the scientific community to study the results and ramifications of what are commonly known as Wolff's laws. One example of this is a 1979 study by Goodship and associates[12] in which unilateral ulnar ostectomies were performed on young pigs in order to cause an increased stress level in the adjacent radius. The animals were sacrificed after three months and cross sections of the radii were taken. It was discovered that in the affected radius, the total area of the bone as well as the area enclosed by the periosteal perimeter increased by a factor of two over the contralateral limb. It was also found that the total area of the hypertrophied radius approached the area of the ulna and radius combined of the contralateral leg.

Another example of the implications of Wolff's laws is shown in a 1978 study by Uhtoff and Jaworski[32] which examined the effect of non-traumatic immobilization of beagle forelimbs. The results of the study showed that bone responded to a dramatic decrease in stress in three stages. During the first six weeks, there was a steady loss of bone mass up to 16 %. The next two to four weeks were characterized by rapid remodelling of the bone up to 10 % of its original mass. In the final stage, the bone underwent slow but persistant loss of bone up to thirty two weeks post immobilization at which time a total of 30 - 50 % of the the total bone mass was absent.

In 1941, C.R. Murray[19] introduced internal fixation of bones using steel plates as a method of treatment for non union fractures of long bones citing their ability to accomplish

"...early reduction with a minimum of violence to bone and soft parts, supplemented by measures designed to reduce pathological reaction in the tissues, as rigid a fixation of the bone fragments as is possible and the institution of active function in all the joints of the part as soon after injury as possible.".

He went on to state reasons why pins and wires, traction-suspension and pin-plaster techniques fail to satisfy these conditions. Further work was done in this area by Horwitz (1945)[13] and Key (1945)[14] who described in detail the operative procedures necessary as well as some qualitative post operative data such as time required before weight bearing could occur. In both of these papers, the authors cited the possibility of infection, the difficulty of the operation, difficulty of removal and the possibility of non-union of the fracture as the primary shortcomings of the procedure.

As mentioned above, the early works on bone plating described only qualitative results and operative techniques, however, Rahn (1971)[21] was succesful in demonstrating that primary bone healing, that is, healing not due to a spanning callus, can in fact be accomplished with the use of steel plates. In this study, adult male rabbit tibiae were osteotomized with a 100 micrometer saw then fixed with plates. The animals were then sacrificed at times ranging from three to nine weeks and longitudinal sections of the tibiae were taken. Rahn stated that the observed remodelling of the Haversian spaces at the site adjacent to the plate, the formation of an interposed layer of tissue at the cortex opposite the plate and the absence of any sub-periosteal callus were evidence of primary healing.

In the late 1960's, concern began to arise about the possible weakening of the healed bone resulting from the use of internal fixation plates with large bending stiffnesses. In 1969, Perren et. al.[20] theorized that reduction of mechanical strain due to excessively rigid internal fixation was the primary cause of spontaneous refracture of bones upon removal of plates.

Cochran[10] measured these strains in plated and unplated bones subjected to physiological loads. Dog femurs were mounted on a special testing apparatus and loads were applied to specimens with and without attached plates. Strains along the bone were collected for over 1000 loading trials. Cochran found that fixing a plate to the bone caused a mean reduction of strain in the bone of up to 45 %, including an 84 % reduction in the region directly beneath the plate.

Prompted by the works of Perrin and Cochran and their study of Wolff's laws, interest in the side effects of rigid internal fixation grew. In 1971, Uhtoff and Dubuc[31] published the results of a study in which they firmly concluded that cortical thinning and subsequent weakening of the bone are a direct result of the stress shunting effected by the application of a rigid plate.

The study consisted of osteotomizing dog femurs, fixing rigid plates to them and examining the healing process at regular intervals from two to twenty four weeks. Careful examination revealed three primary characteristics. The first of these was the discovery that osteopenia had occured in the bone and was most pronounced directly beneath the plate. The second was that a reduction in the diameter of the bone had occured and that this reduction was caused by periosteal resorption. Finally, it was found that there was a persistance of woven bone at the osteotomy implying that normal remodelling of the cortical bone had not occured. All these characteristics increased with time, and diminished upon the removal of the plate, and all were similar to the results observed in cases of non traumatic protection from stress. It was therefore concluded that the application of the rigid plate had caused a rerouting of stress away from the bone, and the subsequent atrophy of the tissue.

It was apparent that stress shunting due to the application of plates with high bending stiffnesses greatly compromised the integrity of the healed bone, so in 1975 Akeson et. al.[1] undertook a study to examine what effects reducing the stiffness of the plate had on the healing process. The material chosen for the study was a graphite-fiber methylmethacrylate resin composite (GFMM). They found that osteotomized canine femurs plated with GFMM plates showed 7% less porosity and over 10% more cortical bone than those plated with Vitallium, a material approximately one order of magnitude stiffer. In a follow up study in 1976, Woo and Akeson[37] took longitudinal sections of bone from similarly treated canine femurs and tested them for strength and mechanical properties. The only significant difference in the mechanical properties of GFMM plated, Vitallium plated or unplated bone was an increase of 12.5% in the strength of the bone plated with GFMM. Similar results were independently obtained and reported in 1976 by Tonino[30] using a plastic polytrifluormonochloroethylene (PTFCE) plate. Both research groups attributed this increase in strength to the fact that more bone mass was retained by the systems plated with the softer material.

It was well documented that bone plates offer the best option for fixation of diaphyseal fractures in many cases (Murray 1941[19]). It was also known that excessively rigid fixation caused various osteopenias (Cochran 1969[10], Uhtoff 1971[31], Uhtoff 1978[32]). It had been shown that plating with more flexible plates resulted in a significantly stronger healed structure (Akeson 1975[1], Tonino 1976[30], Woo 1976[37]). There was also evidence that plating with an excessively flexible material could result in non-union of the osteotomy as well as failure of the plates (Bynum 1971[5], Godfrey 1971[11], Laurence 1969[17], Rahn 1971[21]). What was now needed were analytical and experimental techniques which could yield detailed information about the stress and displacement fields as well as internal forces in the plate bone system, thus allowing examination of the response to variations in material properties, plate geometry, fastener location and loading. Once these relations were established, more effective plating techniques could be developed.

Attempts to analyze the human skeletal system are not new. In 1917, Koch[15] employed beam theory and elementary mechanics in order to determine the internal forces and stresses in the human femur. Koch attempted to show that the stress trajectories in the head of the femur corresponded to the paths formed by groups of trabeculae. Although these findings have since been disputed and modified by modern analytical techniques, Koch's work stands as a breakthrough in the popularizing of mathematical modeling of bones.

In 1972, Rybicki et. al.[25] compared the beam theory solution obtained by Koch to the solution obtained using a finite element method. It was found that in the shaft of the femur, the results corresponded well, but at the head of the femur, an area unlike a slender member and in the proximity of applied loads, the trajectories calculated from the beam model differed significantly from those offered by the finite element analysis.

In 1974, Rybicki[26] employed the same two analytical methods in conjunction with a strain gauge experiment to examine the mechanics of plated fractures. The results Rybicki obtained were among the first of an analytical nature which clearly displayed the stress shunting theorized by previous researchers. It was shown that under compressive loading, certain areas could be shielded from up to 75% of the stress found in the same region of an unplated bone. It is important to note that in his research, only a limited number of cases were analyzed. However, Rybicki stressed that the close correspondence between the analytical and experimental results supported his assertion that beam theory and finite element analysis could be used to examine bone plating.

With advances in finite element software, and the mounting evidence that analytical techniques could yield important data concerning the mechanics of bone plating, papers on the subject began to appear with regularity. In 1977, Simon et. al.[27] conducted a study to try and evaluate the accuracy and practical uses of one, two, and three dimensional finite element models of internal fixation plates by comparing the results of the finite element models with strain gauge measurements. They concluded that in order to obtain accurate information concerning contact stresses, stresses and forces in screws and stresses in areas near fasteners or applied loads, three dimensional models were necessary. If the area of interest was significantly far from any of these locations, one or two dimensional models served equally well.

By the mid 1970's, finite element methods had gained widespread acceptance in the scientific community, including those concerned with the field of Biomechanics. This was due in part to the increase in work on the mathematical foundation of the method, and in part to the repeated successes of the method on problems from a wide range of fields. Researchers now began to exploit the power of computers and software to examine theoretical problems in bone plating.

Woo et. al.[38] conducted an in depth study incorporating both experimental and one dimensional finite element techniques to explore the stresses and remodelling characteristics of bones plated with GFMM compared to bones plated with Vitallium.

Rybicki and Simonen[26] used a two dimensional model to examine the effects of screw angle, plate pretension and end loading due to remobilization. Their model was able to predict with limited accuracy the contact surface of the fracture, as well as the stress distribution on this surface.

In 1984, Cheal[8] carried out a three dimensional finite element analysis of a compression plate fixation system and compared the results to those of a composite beam theory model. The analysis consisted of a greatly simplified quarter symmetric model made up of a limited number of 20 node isoparametric linear elastic elements. The interface between the plate and bone was modelled with one dimensional truss elements thus preventing interpenetration, but failing to allow for stress free seperation of the plate from the bone. The three screws in this system were modelled using three dimensional beam elements. This introduced an incompatibility, but it was considered small enough to ignore due to the high stiffness of the screws. A preload was added to both the plate and the screws, and the model was subjected to a general set of representative loading conditions. For verification of the model, a strain gauge experiment was run in parallel with the analysis and good correspondence was reported.

Among Cheal's findings are three that are of particular interest. First, it was found that although qualitatively, good correspondence between the finite element and composite beam theory existed, the beam model tended to overestimate the shift in the neutral axis which occurs in such a system. Second, Cheal noted that for most load cases, the screw furthest removed from the osteotomy exhibited an increase in shear stresses and bending moments of two to three times over the innermost and middle screws. Finally, the finite element model showed a reduction in stress up to 90 % in the region directly beneath the plate, most prominent near the osteotomy. These results and their implications will be discussed later. The importance of the paper lies in the fact that it clearly demonstrates the ability of a highly simplified finite element model to yield accurate and important results which may point the researcher in the direction of possible problems associated with bone plating, as well as their solutions.

III. BEAM ANALYSIS

The problem examined in this research is expressed for clarity of terms in a simplified diagram (Figure 1). The system consisted of a long bone, 2, severed by a transverse diaphysial osteotomy, 4. The bone is fixed for healing by an internal plate, 1, which is attached to the bone in several places by fasteners, 3, and mounted so that the osteotomy lies directly beneath the center of the plate.

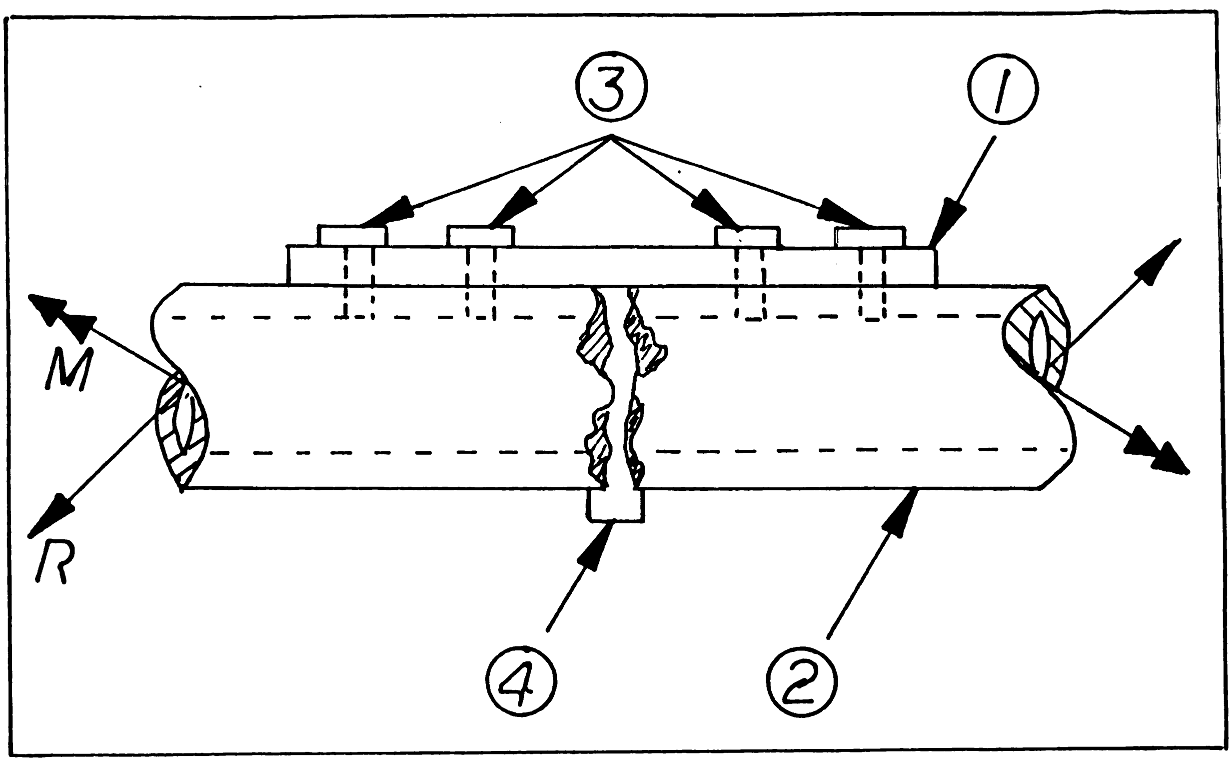

Figure 1. Plated Bone.

The system is subjected to forces and moments which are created by both the external reaction forces resulting from restricted mobilization, as well as the internal forces caused by the flexion and extension of muscle groups in the region.

As a first approximation of the behavior of this system, certain assumptions were made. The bone and plate were treated as slender members subjected to loads causing small deflections. The cross sectional properties of the plate were determined by treating it as a semicircular arc with outside and inside radii of 1.75 and 1.25 cm respectively. The bone was treated as a cirular region with outside and inside radii of 1.25 and .75 cm respectively. The fasteners were modeled as simple Hookean springs having a linear force deflection relationship. The Young's modulus of the plate was given by its manufacturer, and the modulus of bone was taken from Van Buskirk and Ashman[32]. These simplifications allowed the standard moment curvature relations from elementary beam theory to be used.

The osteotomy was treated as a plane of symmetry and the load was considered to be a pure bending moment. With the known material constants and geometric properties (E, I, A, etc.), the resulting statically indeterminate system was formulated and solved as described below (Figure 2).

The moment equations of this system were expressed using singularity functions of order 1, located at l_i to model the moments due to the spring forces.

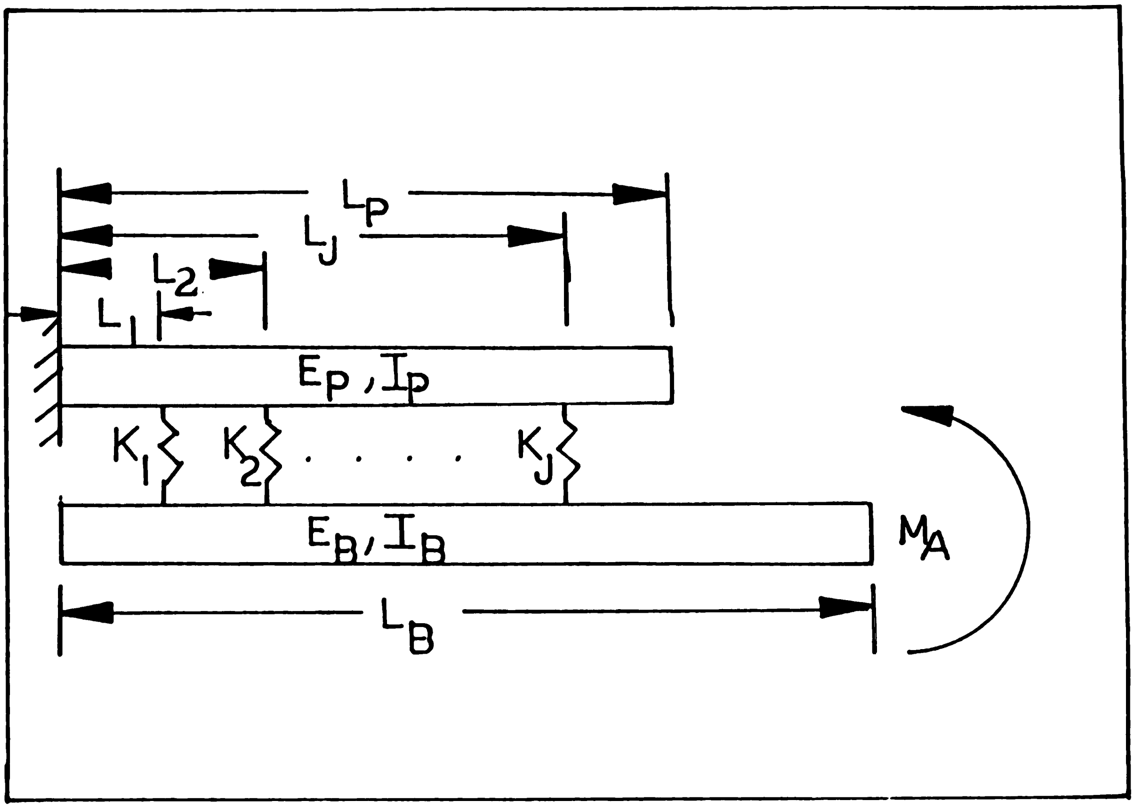

Figure 2. Beam Model.

$$M_p = M_A + Fs_1*<x-l_1> + \ldots + Fs_j*<x-l_j> \tag{1}$$

$$M_b = -Fs_1*<x-l_1> - \ldots - Fs_j*<x-l_j> \tag{2}$$

Integrating equation (1) and imposing the boundary conditions $v_p(0) = v_p'(0) = 0$ yields;

$$v_p = Ma*x^2/(2*E_p*I_p) + Fs_1*<x-l_1>^3/(6*E_p*I_p) + \ldots$$
$$+ Fs_j*<x-l_j>^3/(6*E_p*I_p), \tag{3}$$

and

$$v_b = -Fs_1 * \langle x-l_1 \rangle^3/(6*E_b*I_b) - \ldots -$$

$$Fs_j * \langle x-l_j \rangle^3/(6*E_b*I_b) + C3*x + C4 \qquad (4)$$

The geometric compatability boundary conditions,

$$v_p(l_i) - v_b(l_i) = Fs_i/K_i, \qquad (5)$$

are imposed, yielding:

$$C3*l_i + C4 - \sum_{j=1}^{i-1}[-(l_i-l_j)^3/(6*E_b*I_b) -$$

$$(l_i-l_j)^3/(6*E_p*I_p)] * Fs_j - Fs_i/K_i =$$

$$= Ma*l_i^2/(2*E_p*I_p) \qquad (6)$$

Next, a contact condition which depends on the sign of M_a,

$$v_b(0) - v_p(0) = 0, \quad M_a < 0 \qquad (7)$$

or,

$$v_b(l_p) - v_p(l_p) = 0, \quad M_a > 0 \qquad (8)$$

was added, yielding either:

$$C4 = 0 \qquad (9)$$

or,

$$C3*l_p + C4 + \sum_{j=1}^{N}[\ -(l_p-l_j)^3/(6*E_b*I_b)\ -$$

$$(l_p-l_j)^3/(6*E_p*I_p)]\ *\ Fs_j = M_a*l_p^2\ /(2*E_p*I_p). \quad (10)$$

Finally, force and moment equilibrium were included to add two more equations, where R is the contact force generated.

$$Fs_1 + Fs_2 + \ldots + Fs_j + R = 0 \quad (11)$$

$$Fs_1*l_1 + Fs_2*l_2 + \ldots + Fs_j*l_j + R*l_p = M_a. \quad (12)$$

Thus for n springs, n+3 equations were obtained for n+3 unknowns: Fs_1, Fs_2,..., Fs_n, R, C3 and C4. Solving these equations and substituting into (3) and (4) gave the displaced shape.

To interpret the results from this model, a number of things need to be considered. First, since the spring and the reaction forces were all assumed in compression, a negative sign on any of these indicated a tensile force . Second, since the gap between the plate and bone is assumed to be zero, a compressive spring force actually corresponds to a contact force between the plate and bone. Given an infinite number of springs distributed along the length of the plate, these forces would give a qualitative picture of the pressure distribution on the contact surface for a unit width. Third, geometric arguments reveal that the angle of separation of the fracture, theta, is equal to $\tan^{-1}$ C3, and the downward displacement of the bone, v_o, is equal to C4 (Figure 3). Finally, it can be noted that the displaced shape (Figure 4) has a certain amount of interpenetration.

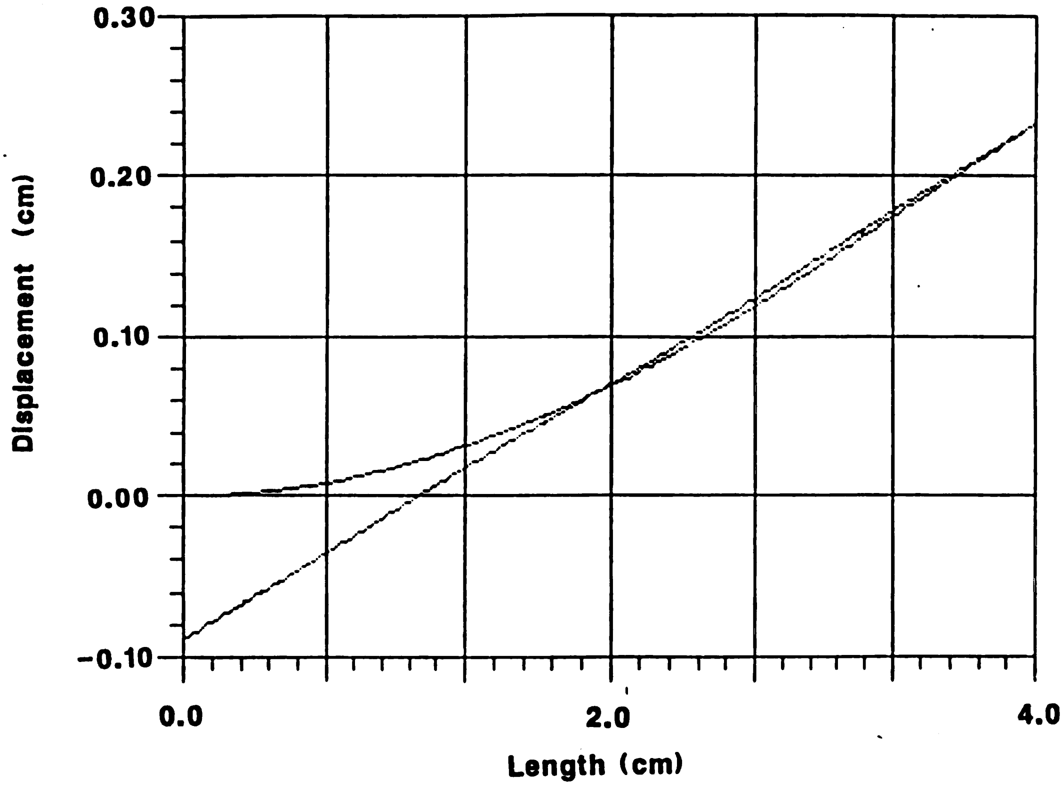

Figure 3. Beam Displacement

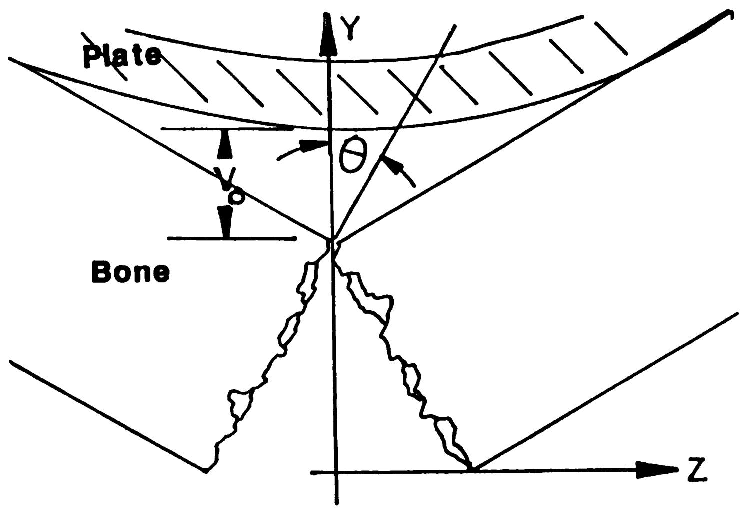

Figure 4. Detail of Osteotomy.

In order to eliminate this, an iterative solution would be needed. In upward bending, the amount of this interpenetration was small and the effect on the solution minimal as evidenced by comparison to experimentally obtained slopes and displacements. In downward bending, however, the interpenetration was extensive and resulted in misleading results. Since the strength of materials model was only a first approximation of the problem, and the iterative solution posed complicated and time consuming problems, the downward bending problem was not solved.

In order to demonstrate the utility of this model, a series of analyses were performed. The value of E_p was varied from 2.65×10^9 Pa to 530×10^9 Pa, 5.3×10^9 Pa corresponding to an actual, tested material, while the rest of the material and physical parameters were held constant.

Figures 5 and 6 show the displacement and slope of the bone at the osteotomy obtained from the beam model, the finite element model, (to be described in the following section), and an experimental study (Melkerson 1987)[18]. It was seen that in the case where experimental data was available, the results of all three methods corresponded well (10 %). It was also seen that the trends exhibited by the finite element model and the strength of materials model were very similar. This was interpreted as verification of the validity of the beam model. It was therefore concluded that if non union of the fracture due to cortical separation in the plane described by the beam model is the primary

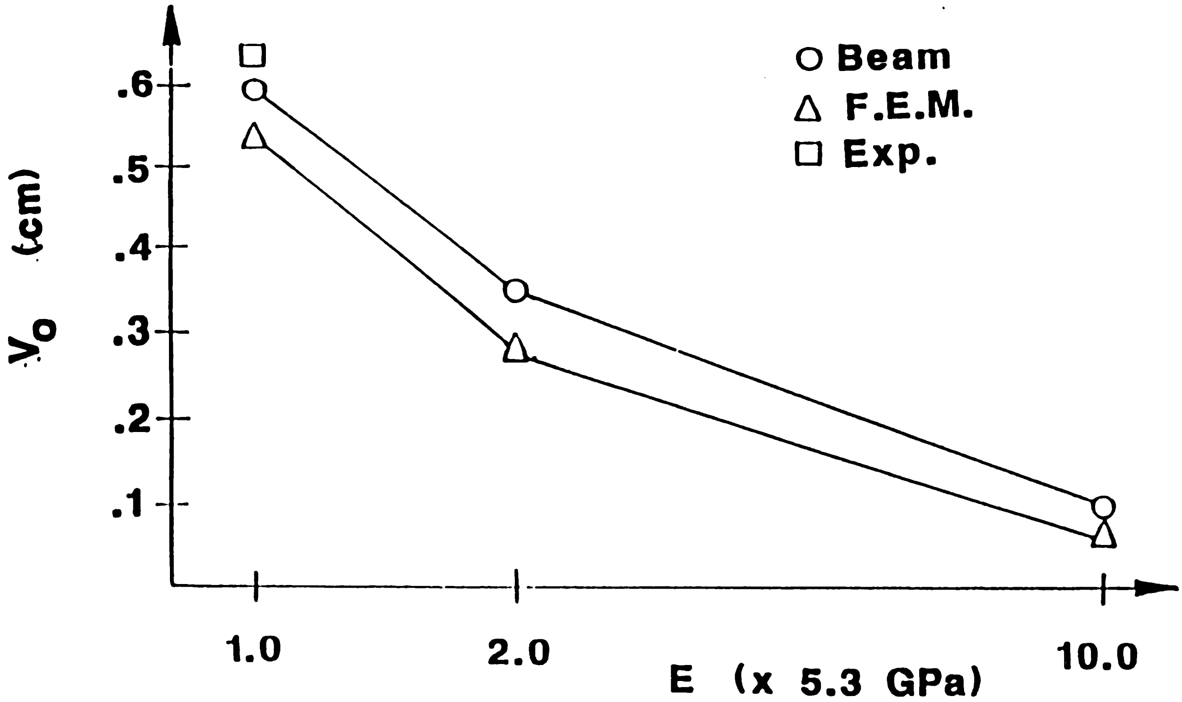

Figure 5. Displacement vs. Stiffness

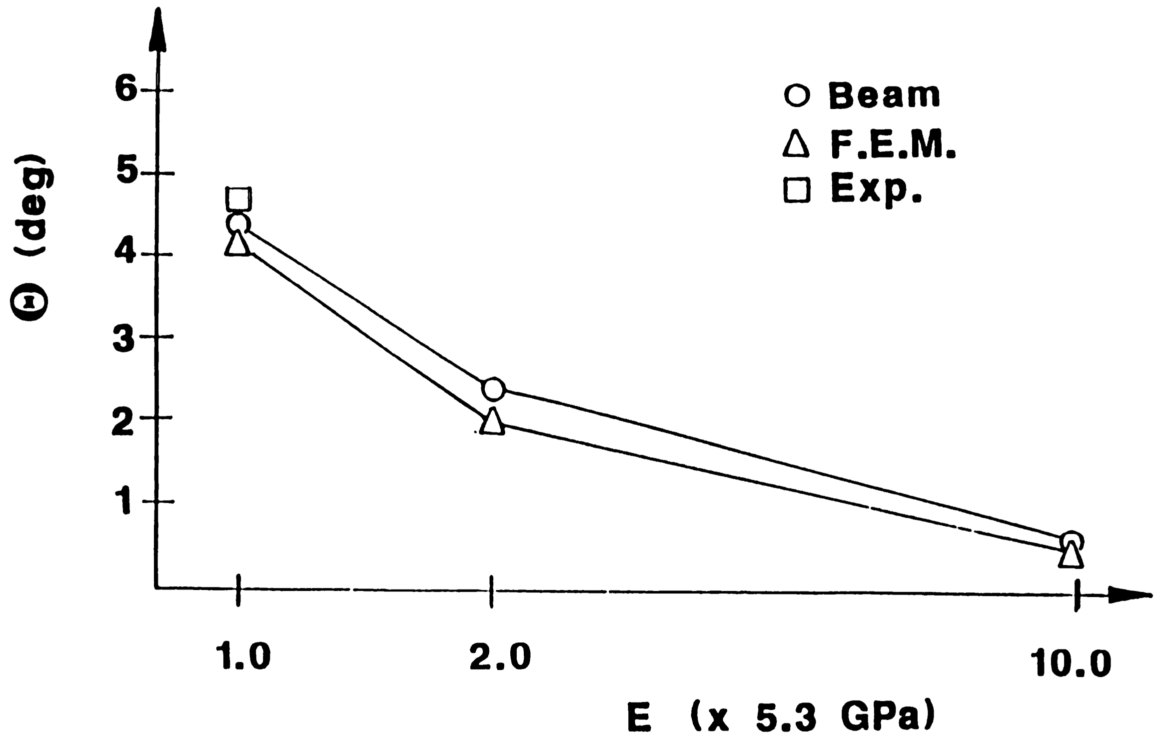

Figure 6. Slope vs. Stiffness

concern of a study, this model is able to yield valuable information needed for evaluation of various plates.

Figure 7 shows the spring forces associated with the analysis described above. It was seen that the spring

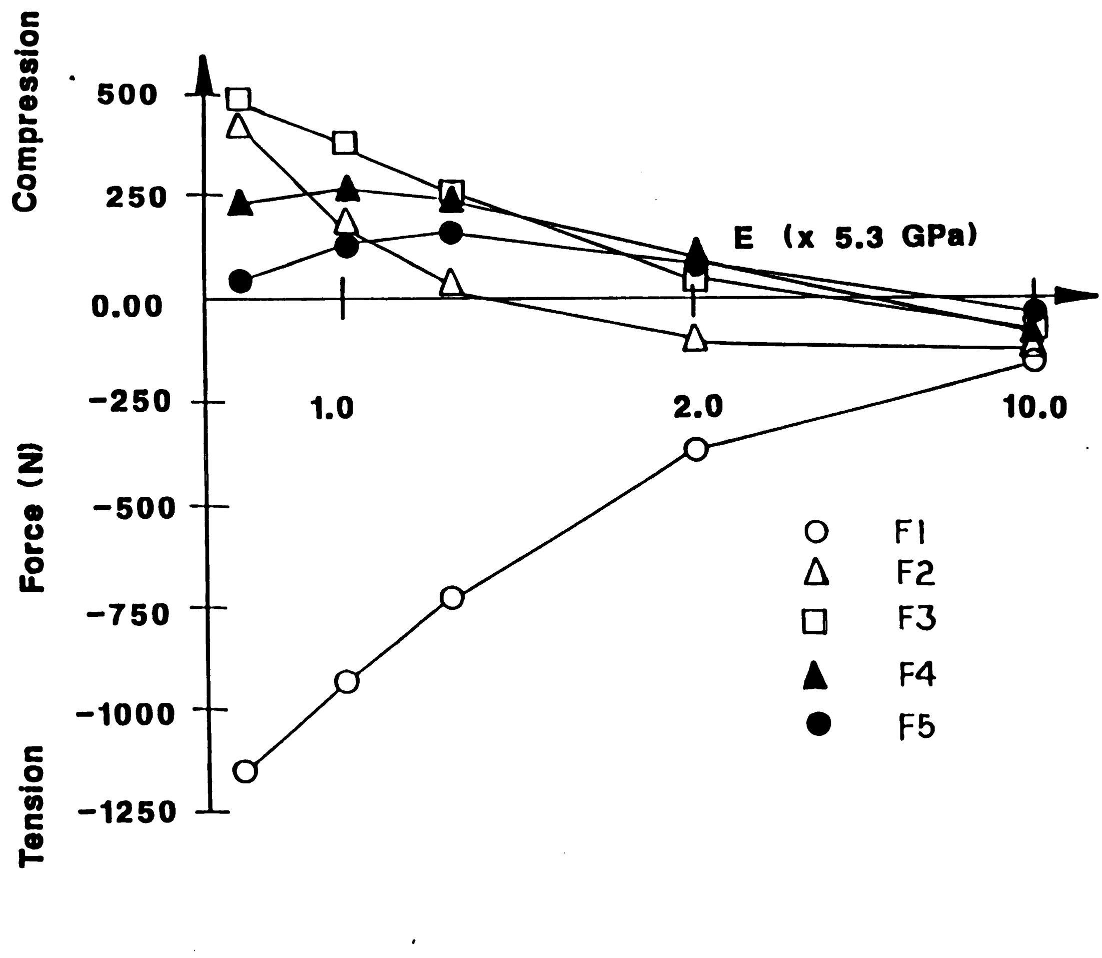

Figure 7. Force vs. Stiffness

closest to the osteotomy, F1, carried the majority of the load on the system. It was also seen that for plate stiffnesses up to 53×10^9 Pa, the rest of the springs were in compression thus implying a contact surface exists in this region of the bone. Finally, it was noted that as the plate increased in stiffness, the forces in the springs approached a linear distribution as would be expected from a simple static analysis.

The beam model indicated that increasing the stiffness of the plate could facilitate the reduction of both cortical separation and fastener forces thus reducing the possibilities of non-union and fastener failure. What is not shown by this model, however, is the stress shielding known to occur under such a modification. It is also not clear from a one dimensional model what effect (if any) fastener pattern may have on out of plane displacements. For these reasons, a more sophisticated model was needed.

Despite some shortcomings, such as the inability to provide stresses, the strength of materials model has a number of useful benefits: it helps to develop a frame of reference for understanding how the system will respond to certain changes in loading, material combinations and geometries; it also yields some basic information about the magnitudes and trends of certain key quantities such as fastener forces, contact forces and the displaced shape of the system. In addition, these results are obtained with virtually no computing costs or time expenditures by the researcher. It is, therefore, deemed to be a useful, albeit crude, design tool.

IV. FINITE ELEMENT ANALYSIS

The second method employed to study the mechanical behavior of the plate-bone system was a three dimensional finite element analysis. The pre-processing, solution and much of the post-processing of the model was accomplished using Swanson Analysis Corporation's ANSYS program, revision 4.2.

The first step in any finite element modelling project is the development of a mesh which gives a converged solution. In mathematics, the term convergence has a number of implications. For example, a continuous function, f(x), can be represented exactly by an infinite series called a Fourier expansion,

$$f(x) = \sum_{n=1}^{\infty}[a_n * \cos(nx) + b_n * \sin(nx)], \quad -\pi \leq x \leq \pi \quad (13)$$

where a_n and b_n are constants. Since this series is uniformly convergent, the truncated series can be examined and written as $f(x) = \sum_{n=1}^{N} [a_n * \cos(nx) + b_n * \sin(nx)] + e(x)$, where e(x) is an error term. An upper bound for the error can then be found and thereby a complete characterization of the accuracy of the finite approximation can be determined (Wienberger)[34]. The creation of a finite element model is analogous to the representation of a continuous function by a truncated series. In the finite element method, a continuous function, displacement, is approximated in a piecewise manner by a set functions of a specified order called shape functions. Elements are simply collections of these shape functions, arranged in a manner to give the proper geometry. Given an infinite number of elements, a representation of the displacement could be obtained accurate to within an arbitrarily small error. For obvious reasons, this is not possible, therefore the analog of a truncated series was created using a finite number of elements. Since the behavior of the solution to a boundary value problem is highly sensitive to the initial conditions, boundary conditions and geometry, it is not possible, in general, to obtain an exact expression for the error introduced by the truncation process. In order to get an approximation of the magnitude and behavior of this error, the technique of mesh refinement is often used (Reddy)[23].

Mesh refinement is the process in which the number of elements in a particular model is increased, and the resulting solution is compared to that obtained from the initial mesh. If key quantities, such as stresses or displacements, do not differ significantly between the two meshes, the model is said to give a converged solution.

In the case of this research, the problem of finding a suitable mesh density was more complicated than aforementioned, since the desire was to create a model which could undergo modifications in its shape, loading and material properties while still yielding a converged solution. Such a model could then be used to assess or develop design modifications by simply stretching, stiffening or reloading it mathematically without having to repeat the whole process of model generation, refinement and verification.

The search for a suitable mesh began with the model depicted in Figure 8 (shaded elements represent fastener location). It had a flat cross section and an

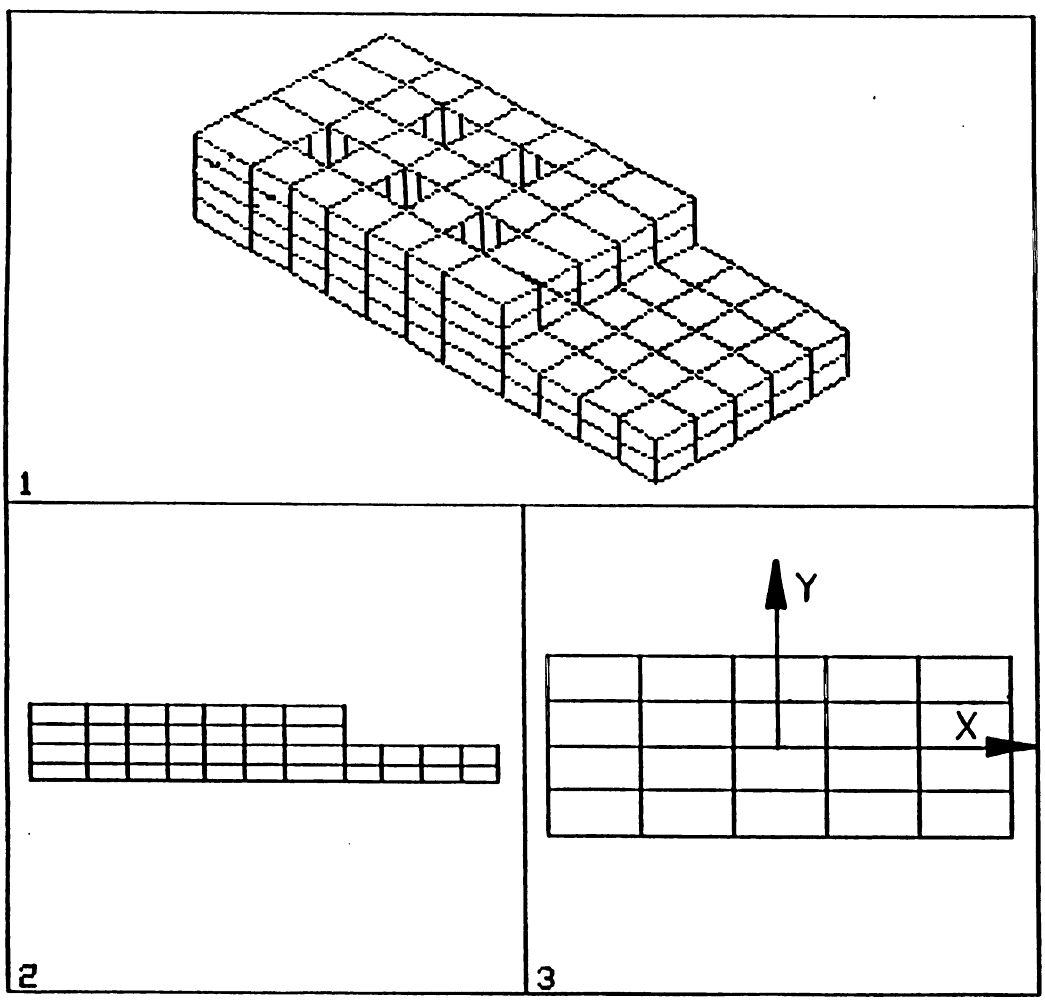

Figure 8. Model 1.

asymmetric fastener pattern. The model consisted of 180 solid elements and 26 gap elements. The gap elements were located at every interface node not occupied by a fastener. In order to mimic the bending response of a curved plate and circular bone, the Youngs modulus of the plate and bone were adjusted accordingly (App 1).

The elements selected to model the plate and bone were ANSYS STIF 45 type. STIF 45 is a three-dimensional, eight node, isoparametric element. The element also contains three nodeless degrees of freedom which allow for a second order shape function in all three directions. This type of element, although nonconforming, has been shown to produce a dramatic increase in accuracy for problems which are loaded primarily in bending (Wilson)[35].

The gap between the bone and plate was modelled using ANSYS STIF 40 combination elements. STIF 40 is a non-linear element, represented schematically in Figure 9. This element was chosen to allow for stress free separation of the plate and bone. In order to accomplish this, STIF 40 requires an iterative solution. When the status (open or closed) of all gaps remains unchanged for an entire iteration, the solution has been reached. For the models to be described, a simple elastic gap was simulated by setting K1 and C were equal to 0.0, and K2 to 200,000 N/m as shown in the verification example provided by Swanson.

Taking advantage of the symmetry and skew symmetry of the problem, only half of the plate-bone system was

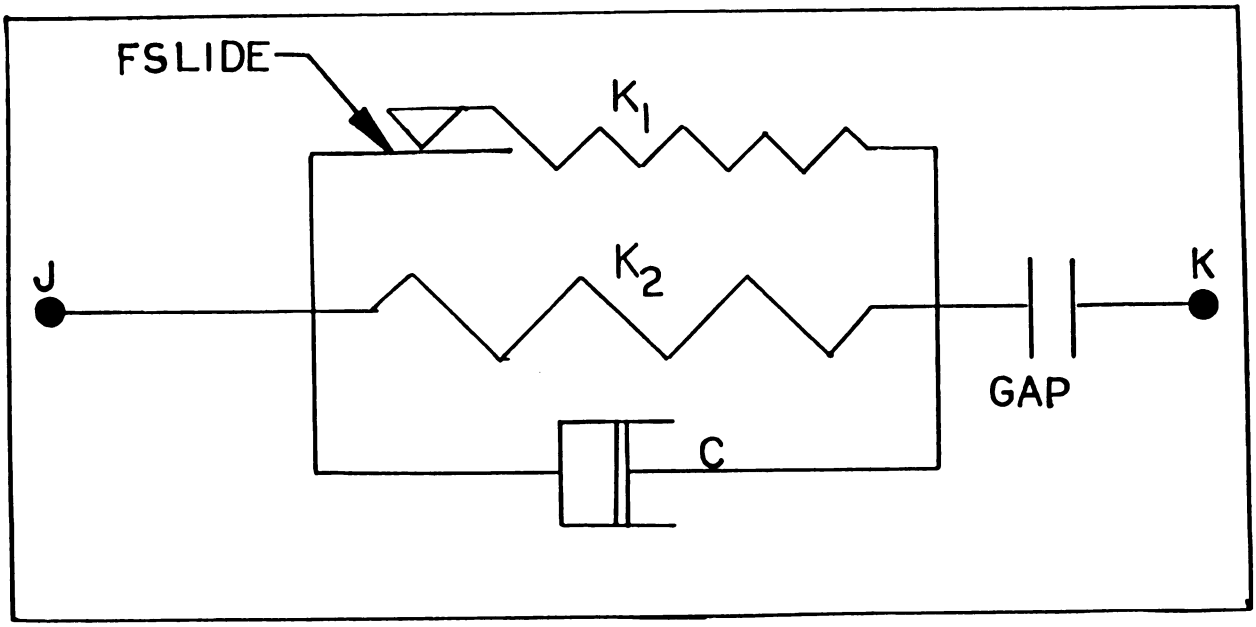

Figure 9. Interface Element.

modelled. The dimensions of the plate were 40mm x 5mm x 25mm, the bone had the same thickness and width, but had an increase in length of 20mm to accomodate for St. Venant's effect.

Displacement boundary conditions were imposed on the system. At the left end of the plate, nodes in the cross section of the plate were constrained in the y and z directions to model the skew symmetry of the system. One of these nodes was further constrained in the x direction in order to prevent any rigid body motions. Nodal forces were applied at the right end of the bone to create a net moment about the x axis, thus modelling the primary moment encountered in vivo.

Three refinements were performed on the initial mesh. The number of elements along the length of the plate was increased from seven, to fourteen, to twenty eight elements, with the accompanying change in the bone. These models consisted of 180, 360, and 720 solid elements and 26, 52, and 104 interface elements respectively. Since the variations in stress through the thickness and across the width of the plate and bone were approximately linear and constant, and the size of the problem was largely a function of the number of nodes in the cross section, the number of elements in these directions was not altered. The second of these conditions was the most important since the available version of ANSYS was not able to accomodate the increase in problem size.

Figures 10 and 11 display the bending stress and y displacements associated with the refinement from the seven to the fourteen to the twenty eight element long model. The line of nodes chosen for the display is at the top center of the plate, adjacent to the row of elements containing three fasteners. The twenty eight element long model was selected over the fourteen element model since it offered an increase in accuracy, especially in the area of the fasteners, with only a moderate increase in computing time.

The next step in the verification process was to change to a more realistic geometry featuring a curved cross section as shown in Figure 12. Once again the Young's modulus of the bone was altered in a similar manner as was

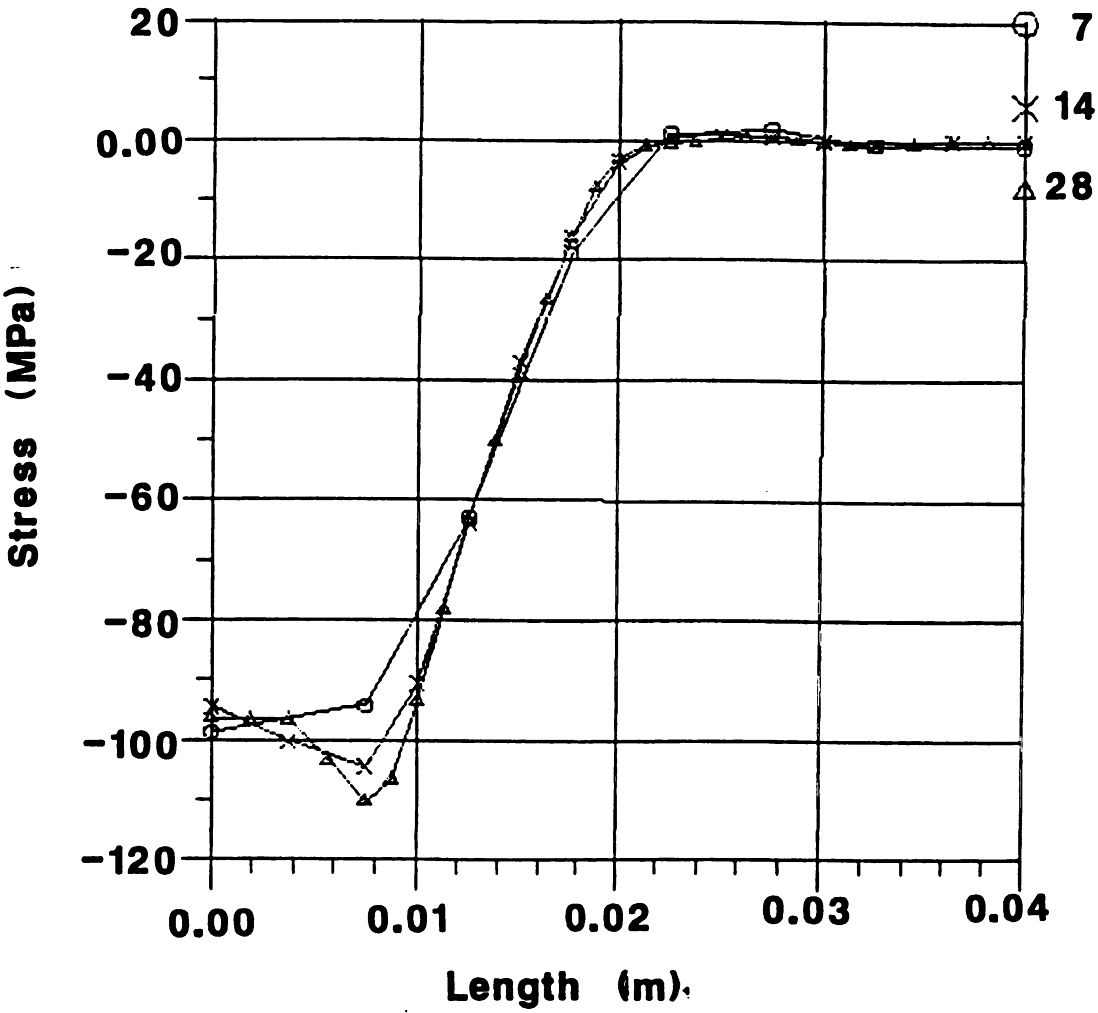

Figure 10. Model 1 Stresses.

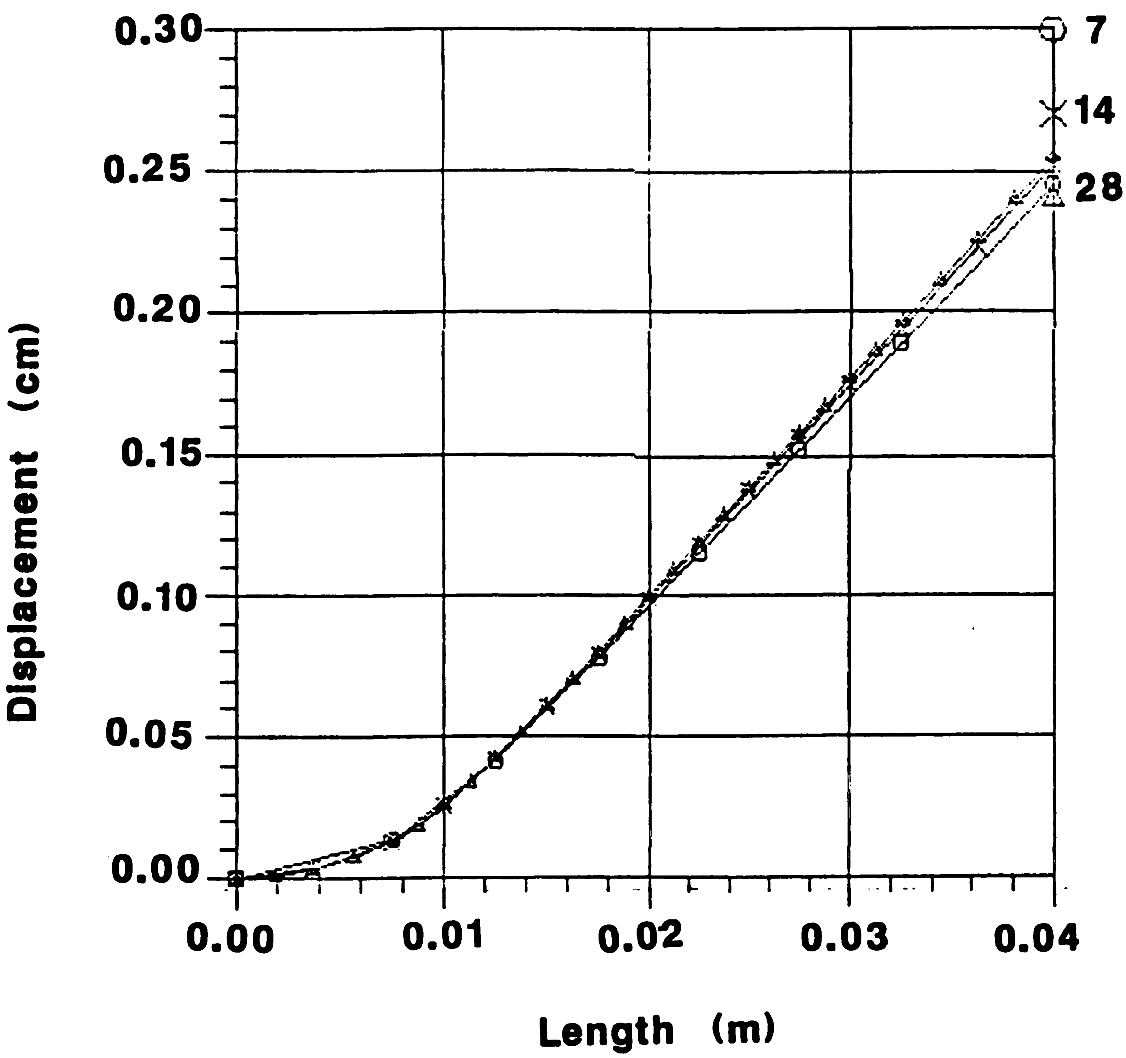

Figure 10. Model 1 Displacements

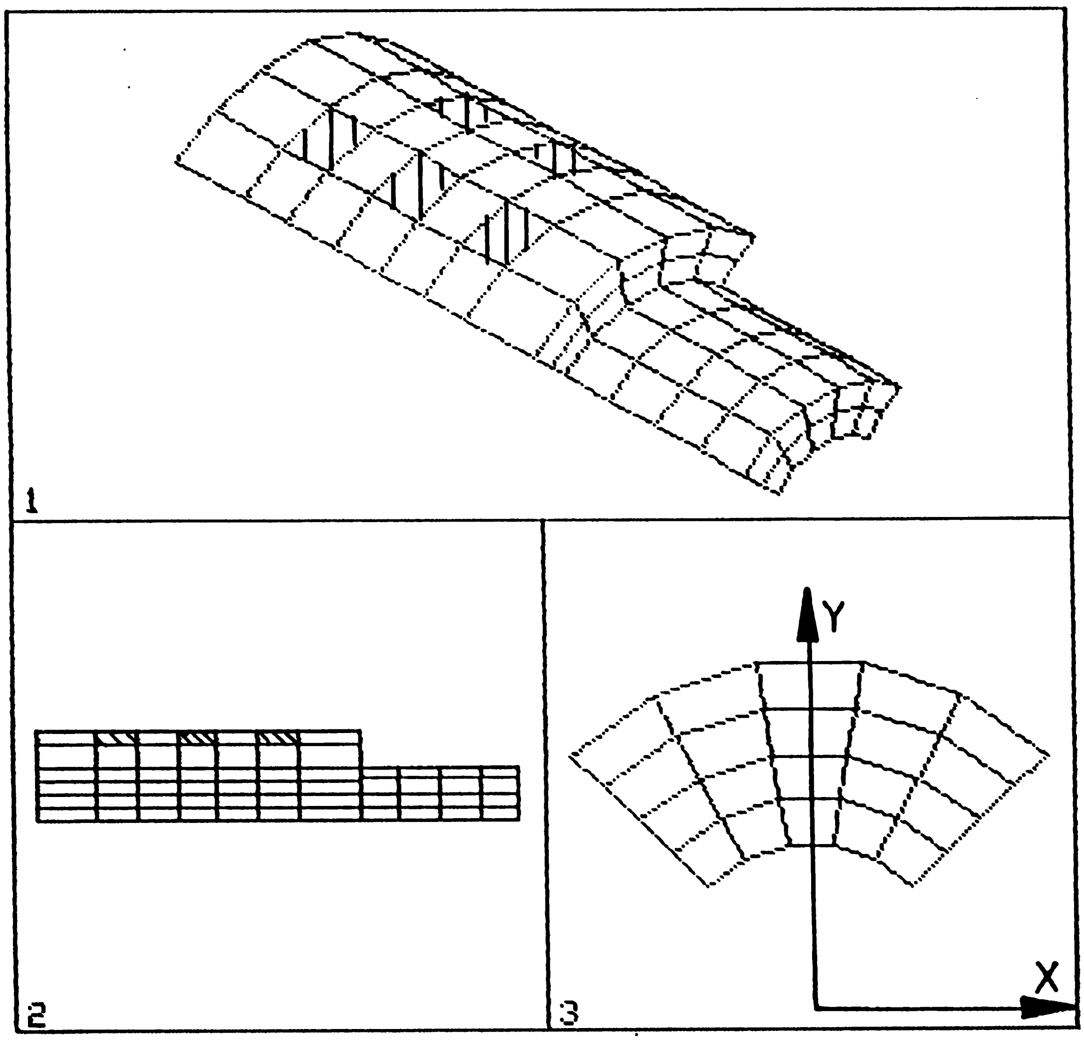

Figure 12. Model 2

described earlier. Since the plate was now depicted by its proper cross section, its modulus needed no adjustment. Figures 13 and 14 display stresses and displacements for the fourteen and twenty eight element long models for the new, more realistic model. It was found that for the new.

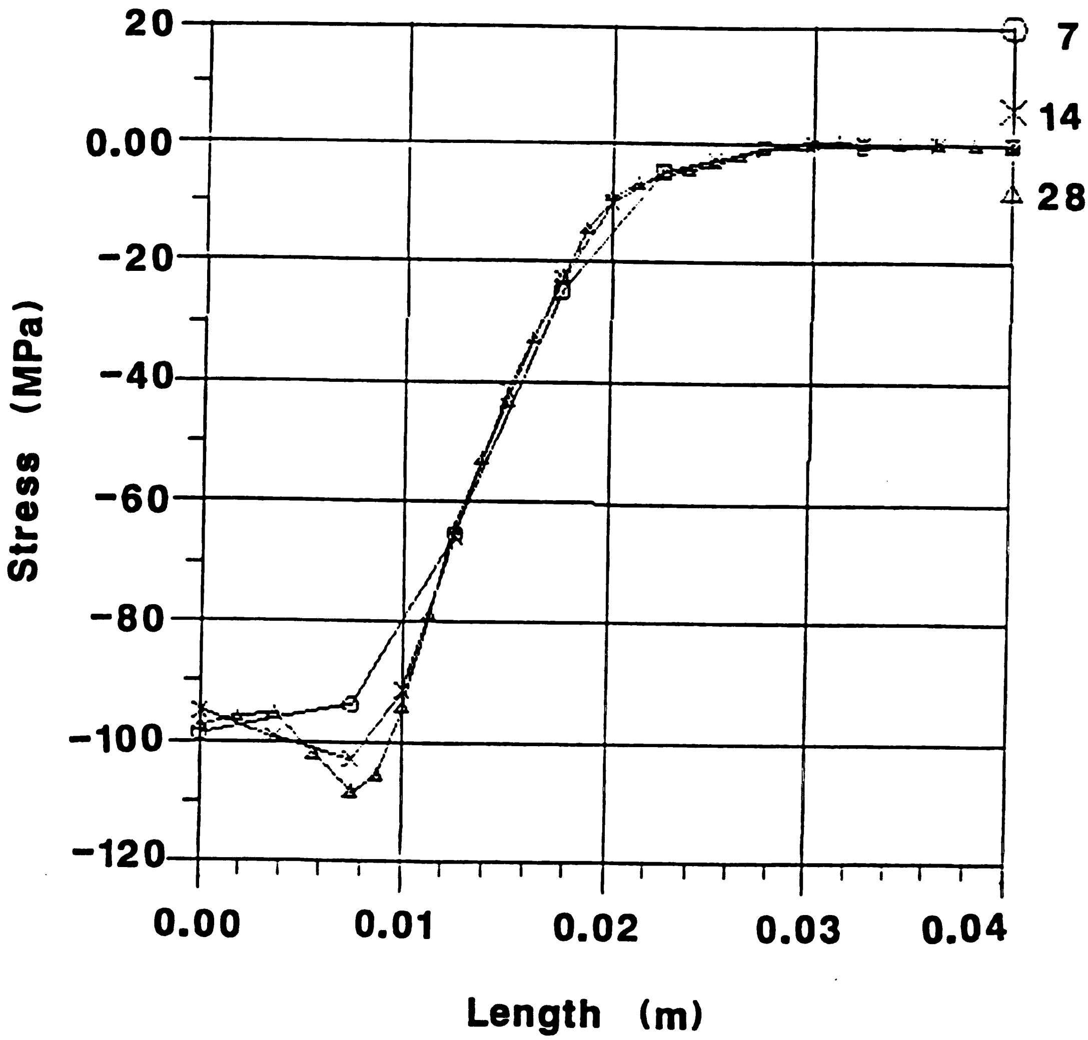

Model 2 Stresses

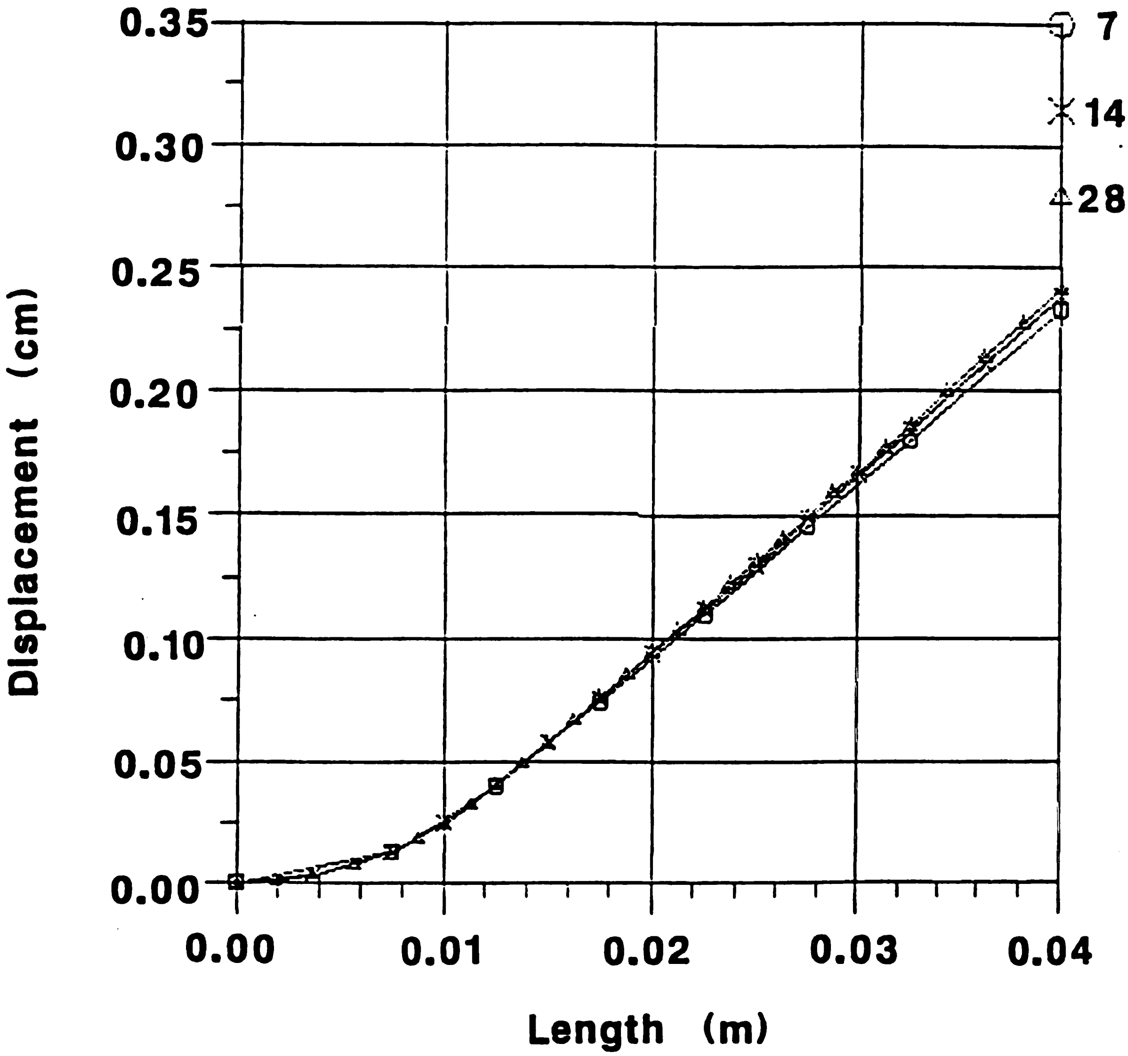

Figure 14. Model 2 Displacements

geometry, no increase in mesh density was needed to obtain a converged solution.

The final step in the development of the finite element model was the completion of the bone cross section so that it corresponded to the actual shape. The reason for this was that although the bending response of the system could be adjusted by varying the Young's modulus of its components, the stress response, and in particular, the shift of the neutral axis, would be distorted by the difference in centroidal location between a semi circular arc and a complete circle.

In order to accomodate this change in the mesh while remaining within the size limits of the available processor, certain modelling compromises were necessary. The first of these was a decrease in the density of the mesh in areas not adjacent to the plate. In this region, the elements were increased in size over their neighboring elements by 17 degrees in their angular span, .0025m in their radial span. The resulting model, shown in Figure 15 , was hypothesized to give an increase in the accuracy of the solution in and directly beneath the plate due to the geometrical arguments given above. In addition, the solution in the rest of the bone, although quantitatively suspect due to the sparsity of elements, would, never the less, be qualitatively correct. This modification was therefore deemed acceptable since the areas in which stresses were the primary interest were the

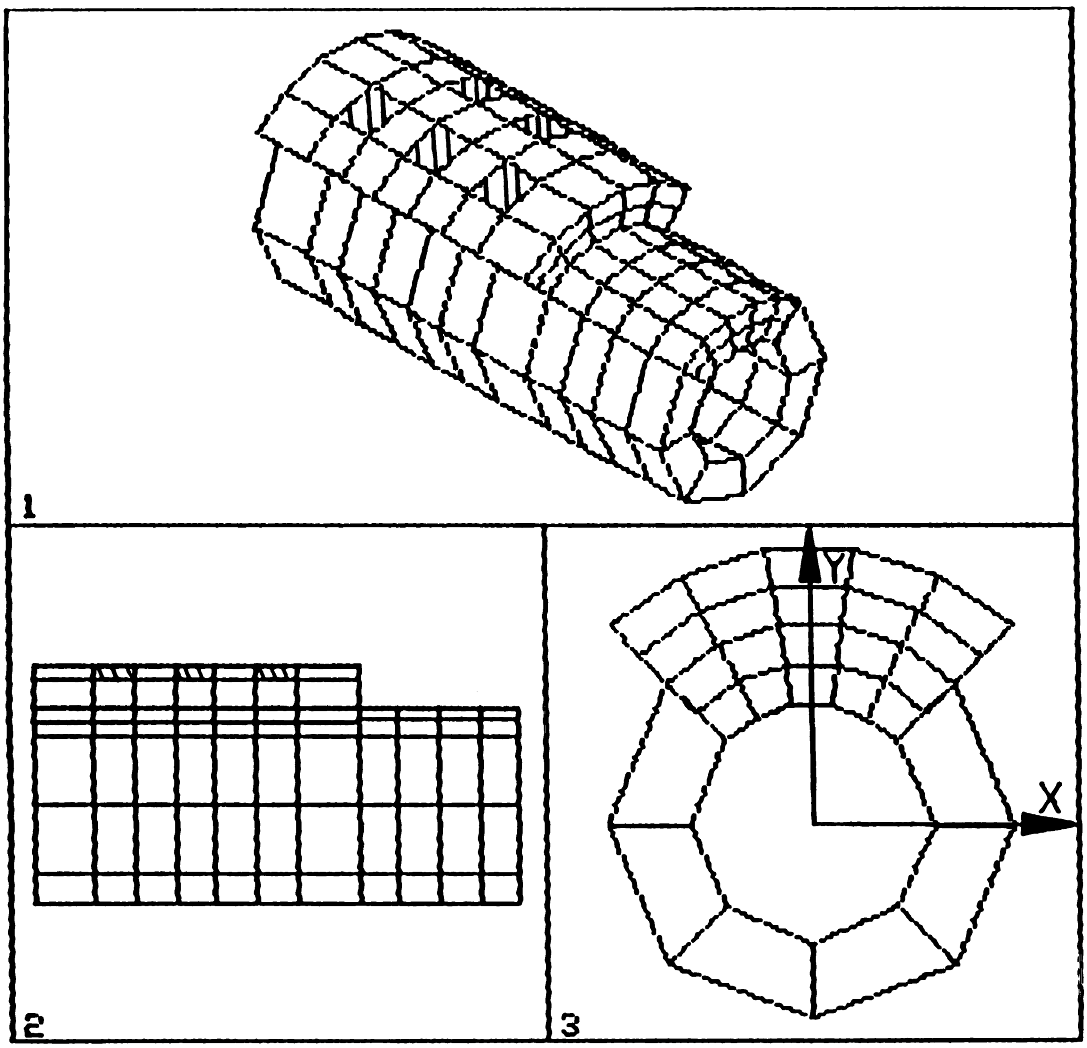

Figure 15. Model 3.

plate and the part of the bone directly beneath it (Cochran 1969[10], Rybicki 1974[26], Uhtoff 1971[31]).

The second, and more serious modelling compromise, caused by size limitations, was the creation of 'free nodes' upon refinement of the mesh (Figure 16). In order to

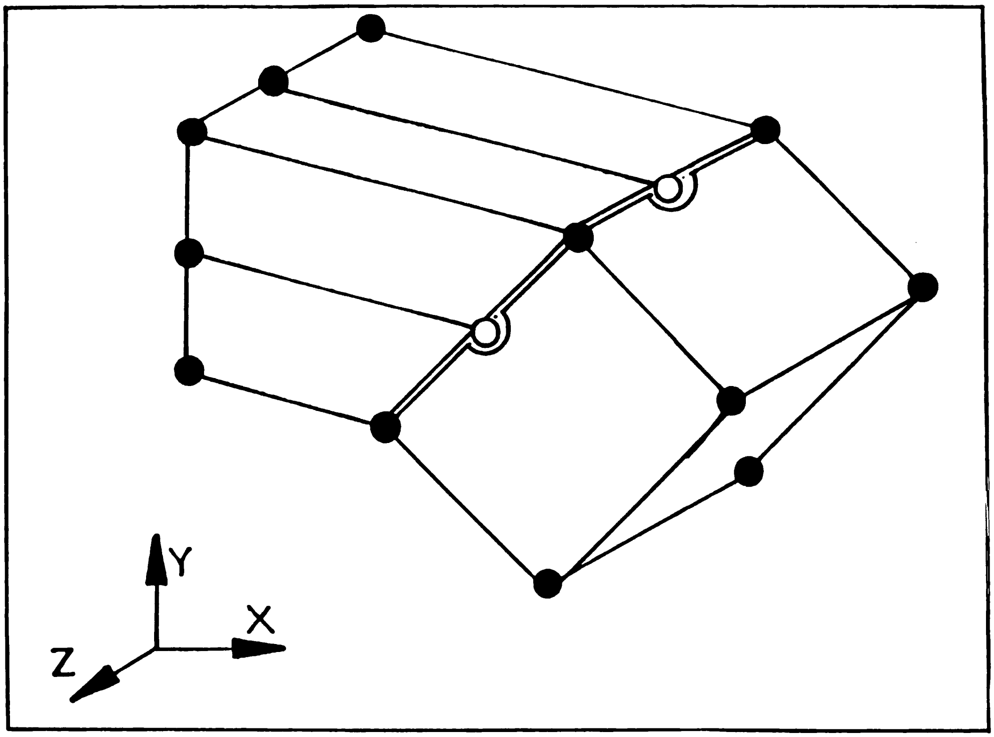

Figure 16. Free Nodes.

determine the extent of the error caused by the free nodes, a number of them were examined in detail.

Characterization of the exact effect of these free nodes would be nearly impossible, so in order to get an idea of the amount of error involved, a quantity which will be referred to as incompatible shear was defined and calculated as follows. The xy components of this shear are shown in Figure 17 as phi and psi, and can be interpreted as follows:

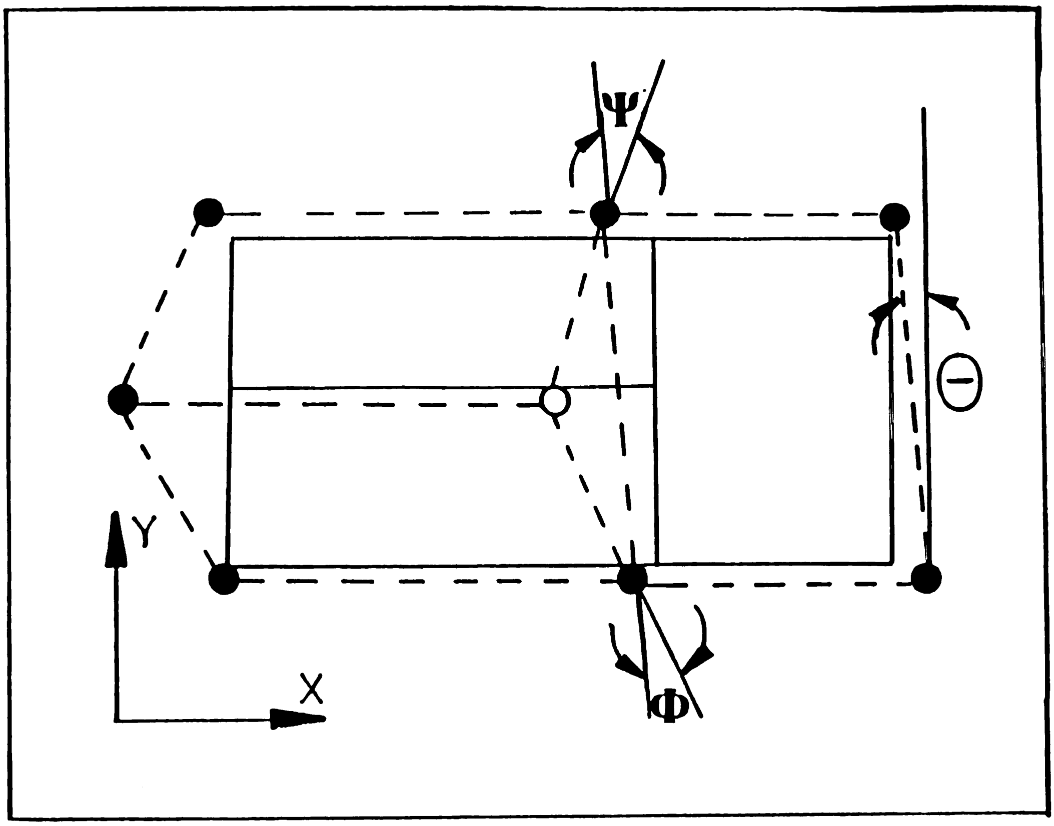

Figure 17. Incompatible Shear

if the free node, marked by an open circle, had been attached to element 3, the entire group of elements would have sheared by an amount theta. Since the free node is unconstrained, it displaces thus creating the incompatible shears.

A number of such groups of elements were examined and the incompatible shear in all planes was found to be on the order of 10% of the total shear (max(phi,psi)/(theta)). It is difficult to gauge the importance of this number, however, there are reasons to feel that it is in an acceptable range. First of all, the shear stress in this region is not of great importance as it is in the bone and far removed from the fasteners. Second, the region where free nodes occur is confined to two lines of nodes, and the rest of the model is free of this type of incompatibility. Given a larger processor, this type of modelling would be discouraged, but in light of the limitations imposed in this case, it seems to be a reasonable approach.

Repeating the mesh refinement process described earlier, Figures 18 and 19 were obtained. Displayed are the stresses and displacements described for previous models. Another consideration in the verification of the model was whether or not the converged solution corresponded to experimentally obtained data. No quantitative stress data were available, however it was known from experimental studies, both in vivo and in vitro, that failure of the plates was often initiated at the outside of the fastener closest to the osteotomy(Melkerson[18]). The finite element model predicted maximum tensile stress at the nodes corresponding to this location. Another measure of the correlation between the model and the actual system was the displaced shape of the system, which was very accurate as

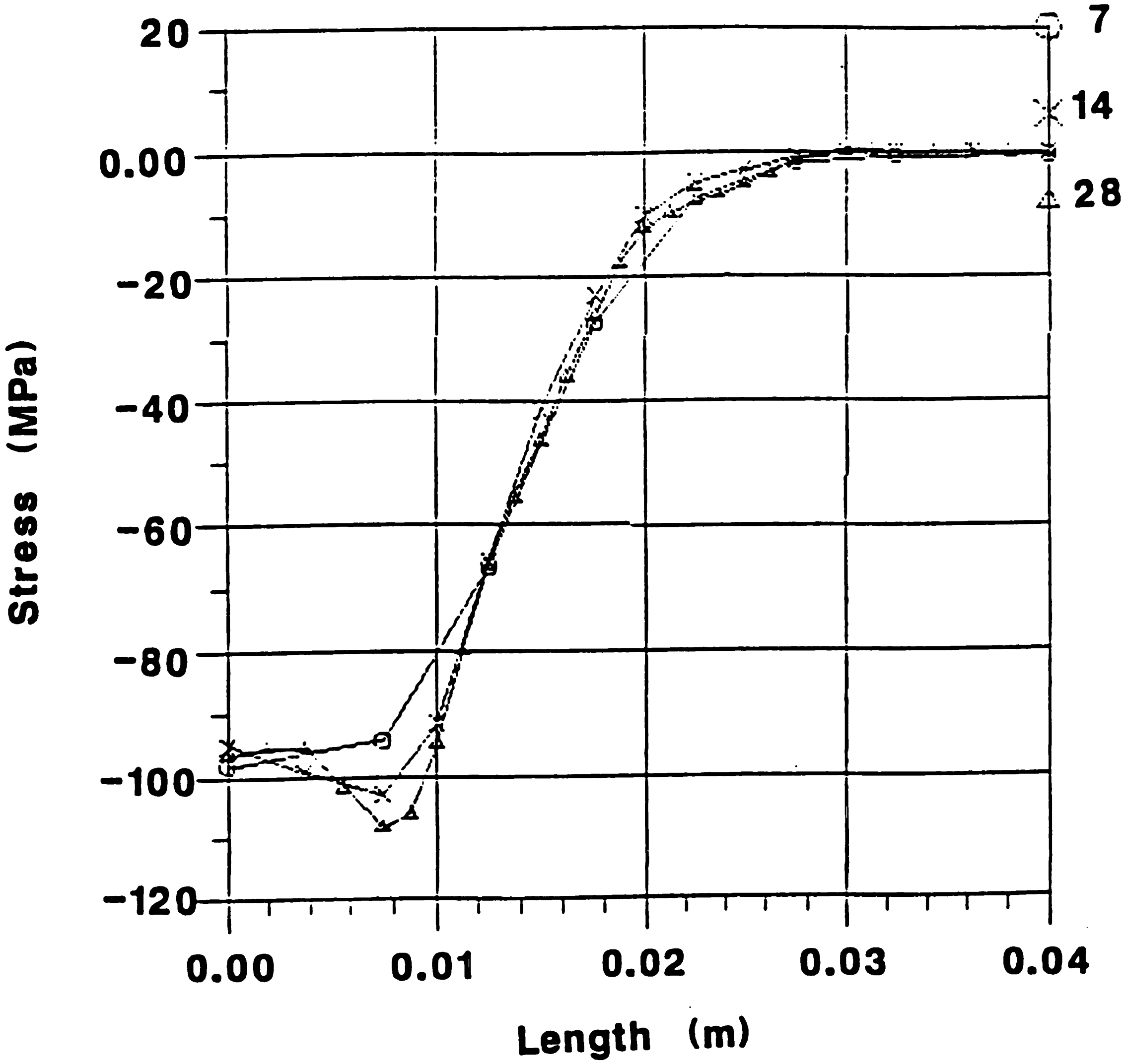

Figure 18. Model 3 Stresses.

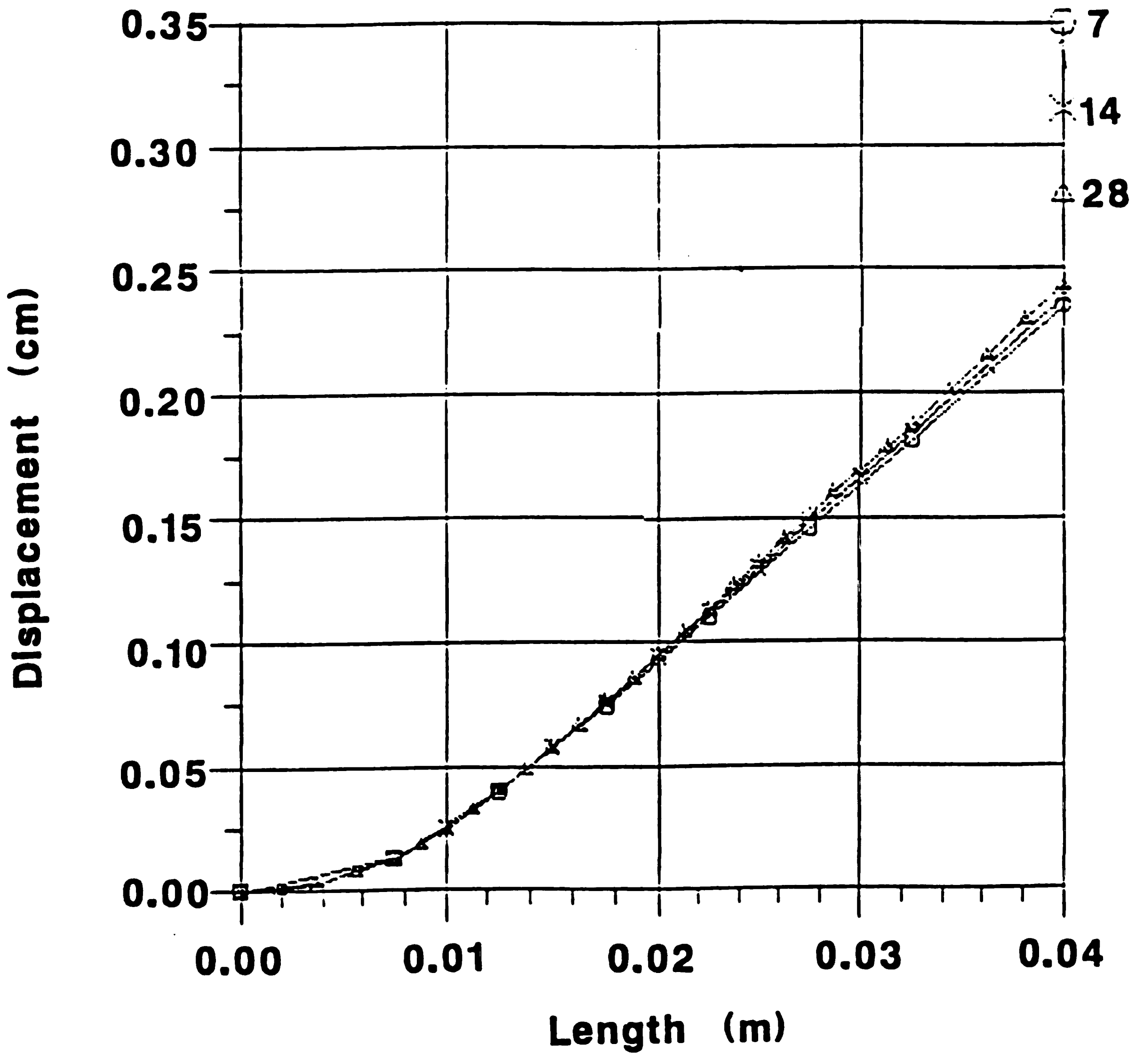

Figure 19. Model 3 Displacements.

would be expected since finite element analyses based on a displacement formulation generally yield very accurate displacement results.

The results of the verification process indicated that the final finite element model yielded accurate results for the stresses and displacements over a wide range of material properties, geometries and loads. It was, therefore, concluded that the model could be used to examine in detail the mechanical response of plated fractures under a variety of loads, plate materials and geometrical alterations. In the following sections, the power of the model will be demonstrated through a number of examples.

V. RESULTS AND DISCUSSION

There are four primary ways in which failure of a plated bone can occur:

1. Fracture of the plate or bone due to excessive stress.

2. Fracture of the bone due to atrophy caused by stress shielding from plates with high bending stiffnesses.

3. Failure of the fasteners by either excessive stressing or pullout.

4. Non union or poor union of the osteotomy due to excessive motion.

For an analytical model to be of use in the analysis of bone plating, it must be able to yield information pertaining to all of the aforementioned modes of system failure. In order to demonstrate the ability of the finite element model developed in this research to do just that, a number of situations involving load and material property alterations were analyzed.

The first set of results, displayed in Figures 20 through 23, show the primary stress (bending / σ_{zz}) on cross

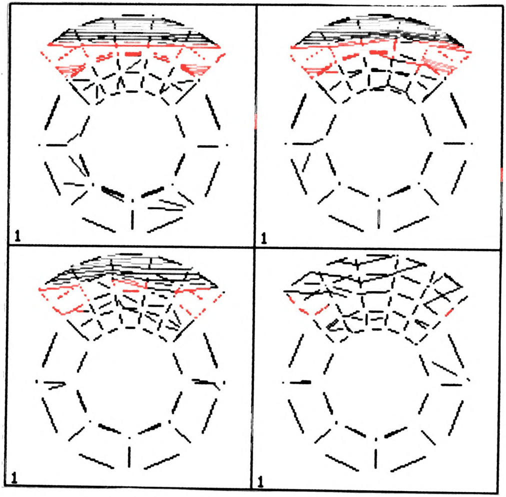

Figure 20. Bending Stress (up)

Scale: -110 MPa 110 MPa

(Dk. Blue) (Red)

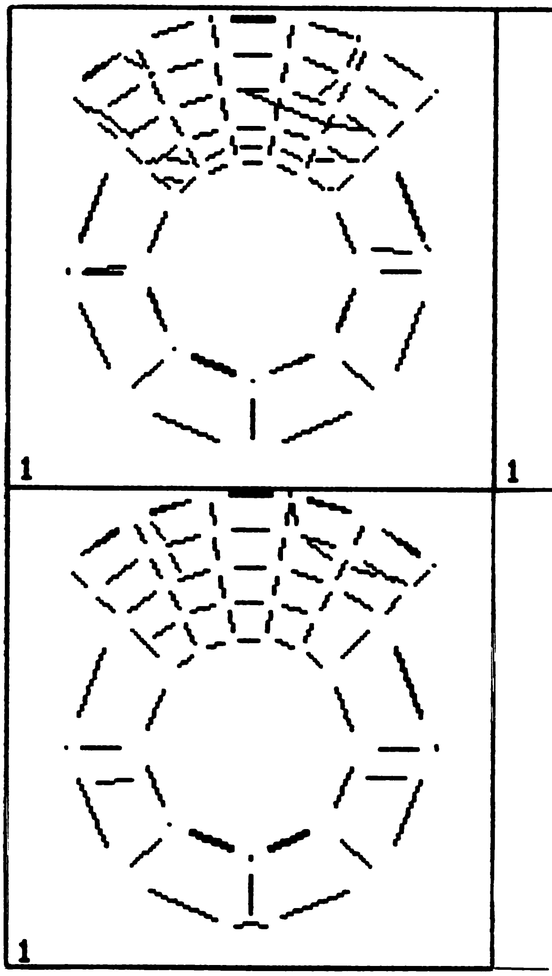

Figure 21. Bending Stress (up)

Scale: -110 MPa (Dk. Blue) 110 MPa (Red)

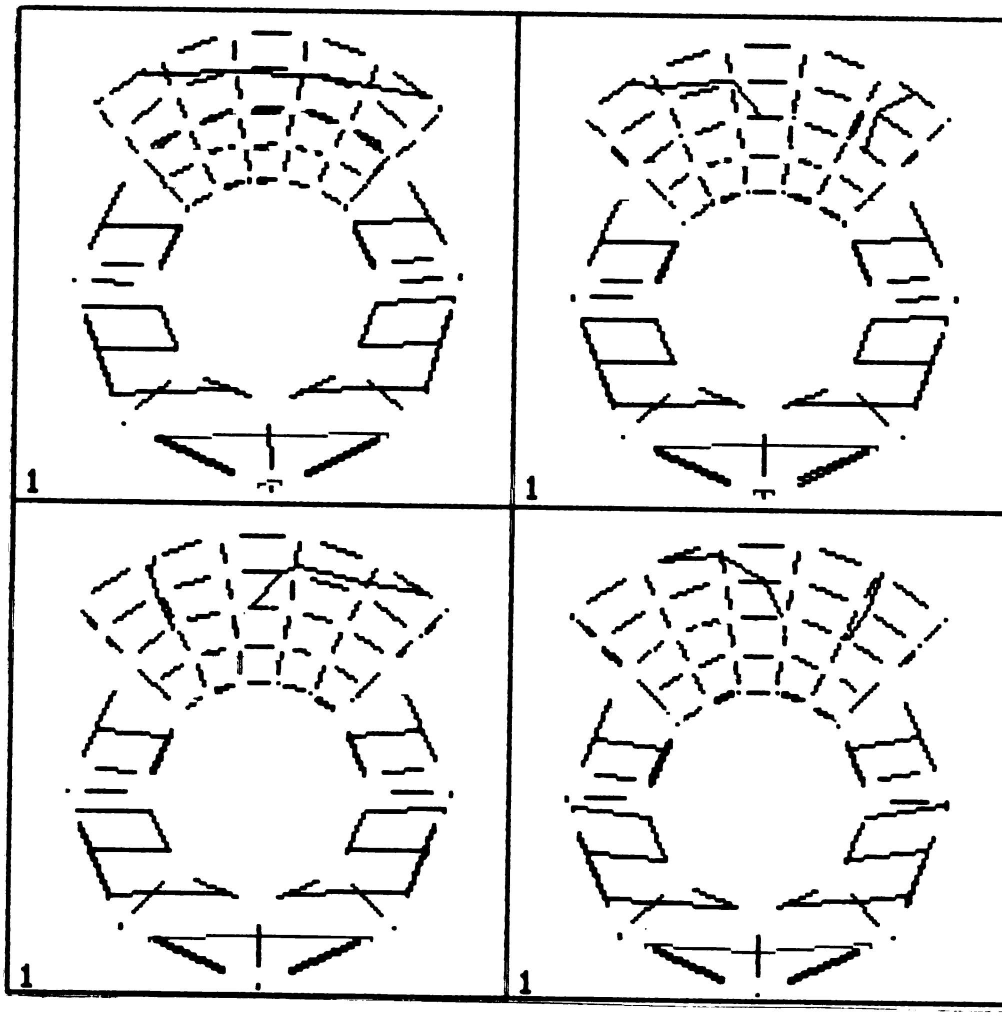

Figure 22. Bending Stress (down)

Scale: -14.5 MPa 14.5 MPa

(Dk. Blue) (Red)

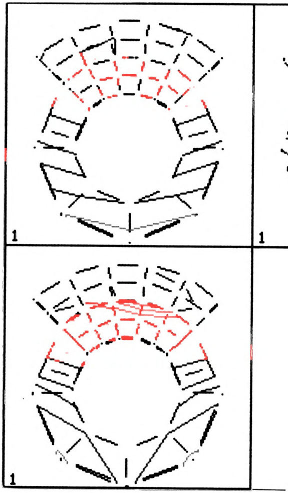

Figure 23. Bending Stress (down)

Scale: -14.5 MPa (Dk. Blue) 14.5 MPa (Red) sections taken every .5 cm (.125 * L_p), along the length of the plate, for upward and downward bending moments of 10 N-m. The Young's modulus for the plate in these figures is 5.3 x 10^9 Pa.

For the upward bending mode, the nodes at the osteotomy were allowed to displace freely, thus modelling a newly fractured bone. For the downward bending mode, the nodes at the osteotomy were constrained in the axial (z) direction, thus modelling a healed bone. These two conditions yield the worst case scenarios for failure types 1 and 2 respectively. A newly fractured bone cannot carry axial tension, thus the plate is exposed to an extreme tensile load. A healed bone is able to carry axial loads, thus the stress shielding found for this physical condition is the important quantity to examine.

Since the primary loading on the system is bending, tensile failure due to high bending stress would be the likely cause of type 1 failure. It can be seen that for upward and downward bending, the maximum tensile stress occurs near fastener 1 and fastener 5 respectively. It is also seen that the magnitude of this stress is approximately seven times greater in upward bending.

The values of the maximum bending tensile stresses in the plate and bone, 110 MPa and 15 MPa respectively, along with the ultimate tensile strengths of these materials, are the quantities needed to determine the possibility of type 1 failure. It should be noted that the problem size limitations restricted the mesh density around the fasteners, and therefore, stress concentrations are not represented by the maxima obtained from this model.

The next figure (Figure 24) displays the bending stress at the osteotomy for downward bending load of 10 N-m and a range of plate moduli: 2.65, 5.3, 10.6 and 53.0 x 10^9 Pa.

Historically, the emphasis in bone plating analysis has been placed on the role of stress shunting, known to be the

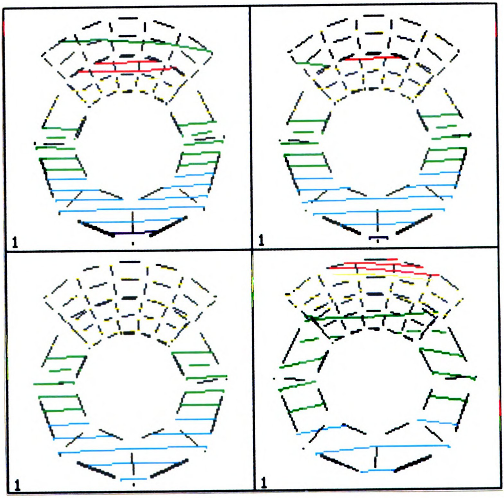

Figure 24. Stress Shunting

Scale: -8 MPa 8 MPa

(Dk. Blue) (Red)

major cause of type 2 failure. This stress shunting is clearly seen at the cross section shown, which is known to be the primary area of bone atrophy. The magnitude of the maximum bending stress in this region of the bone drops steadily from 4 MPa to approximately zero for the given increase in plate modulus from 2.65 GPa to 53 GPa. The model would allow a similar analysis to be performed for any region of the bone under a wide range of loads and plate moduli.

In Figures 25 through 28, the shear stress, σ_{xz}, and normal stress, σ_{yy}, in the fasteners are displayed for loads of plus and minus 10 N-m. The modulus of the fasteners is equal to the modulus of the plate, 5.3×10^9 Pa in this case.

These stresses can be used as a criterion for judging the possibility of tensile, shear or pullout failure of the fasteners. Of particular interest is the occurence of an xz shear. Under the applied load, the likely origin of this stress is torsion of the fasteners, induced as a result of their asymmetric pattern. Although the magnitude of this stress is relatively small for the given load, material and fastener pattern displayed, other combinations of these parameters could result in much larger, and potentially failure causing magnitudes.

The normal stress shown occurs as a result of the fasteners bending in the yz plane and extending or compressing in the y direction. A large positive magnitude of this stress would indicate the likelihood of both pullout of this stress would indicate the likelihood of both pullout

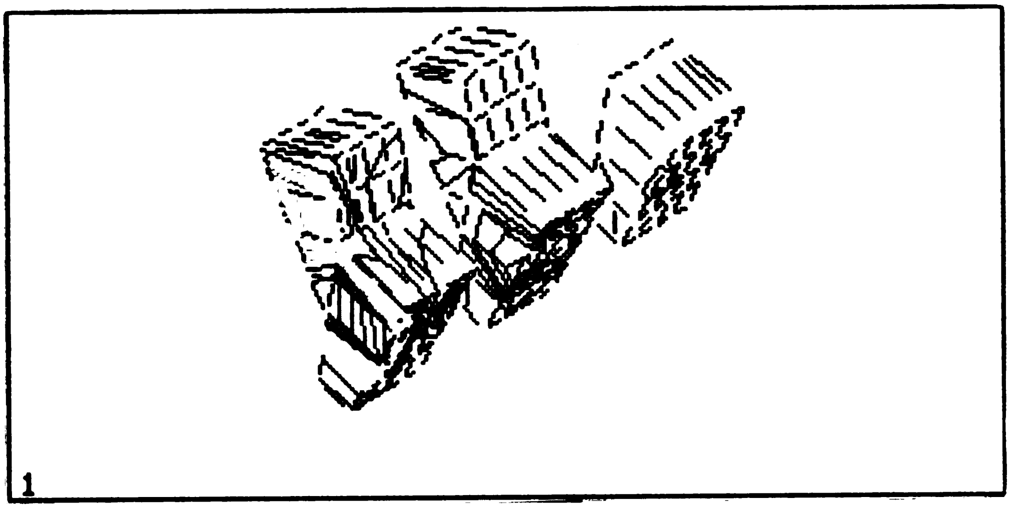

Figure 25. Fastener Stresses, (up, σ_{yy})

Scale: -100 MPa 100 MPa

(Dk. Blue) (Red)

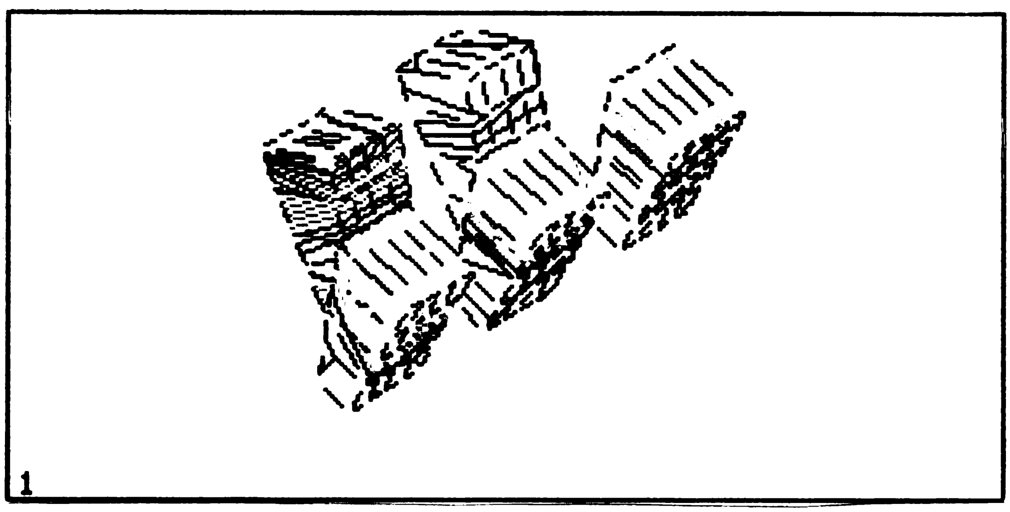

Figure 26. Fastener Stresses (up, σ_{xz})

Scale: -13 MPa 13 MPa

(Dk. Blue) (Red)

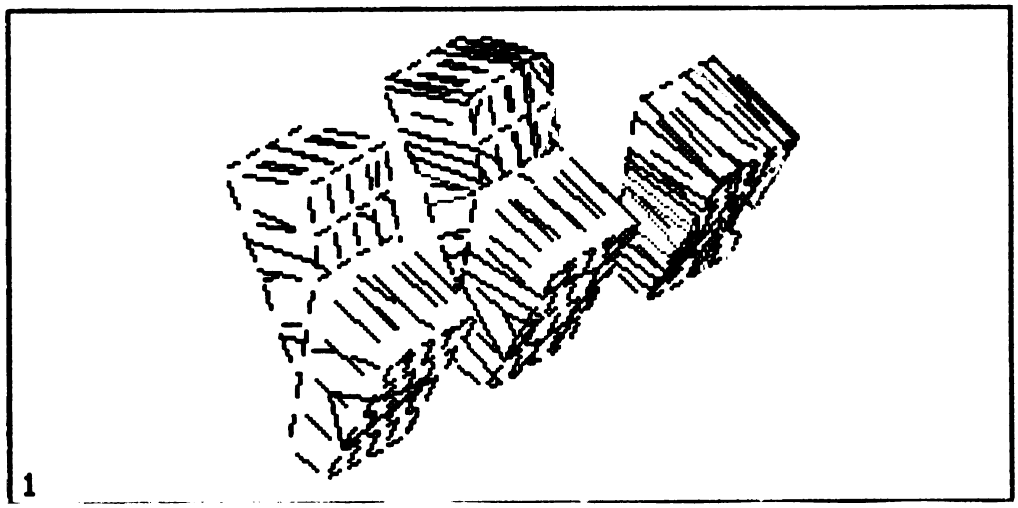

Figure 27. Fastener Stresses (down, σ_{yy})

Scale: -2.5 MPa 2.5 MPa

(Dk. Blue) (Red)

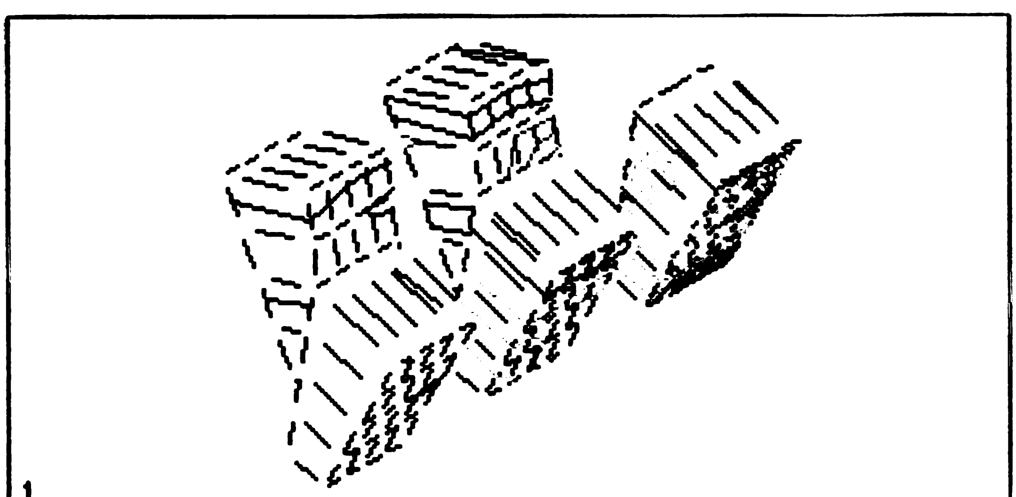

Figure 28. Fastener Stresses (down, σ_{xz})

Scale: -1.0 MPa 1.0 MPa

(Dk. Blue) (Red)

and tensile failure of the fasteners. It is important to notice that there is a definite reversal of fastener load bearing between upward and downward bending of the bone. This is in contradiction with the results reported by Cheal[8]. The most likely causes of this discrepancy are Cheal's use of one dimensional beam elements to model the fasteners and the inability of his model to allow stress free seperation of the plate from the bone.

The in plane displacements of the bone at the osteotomy were available from the strength of materials model and were presented earlier along with the corresponding results from the finite element model. The out of plane angular displacement, however, is a three dimensional quantity, and therefore, could not be seen in the results of the beam model. Figure 29 depicts this angle for clarity, while

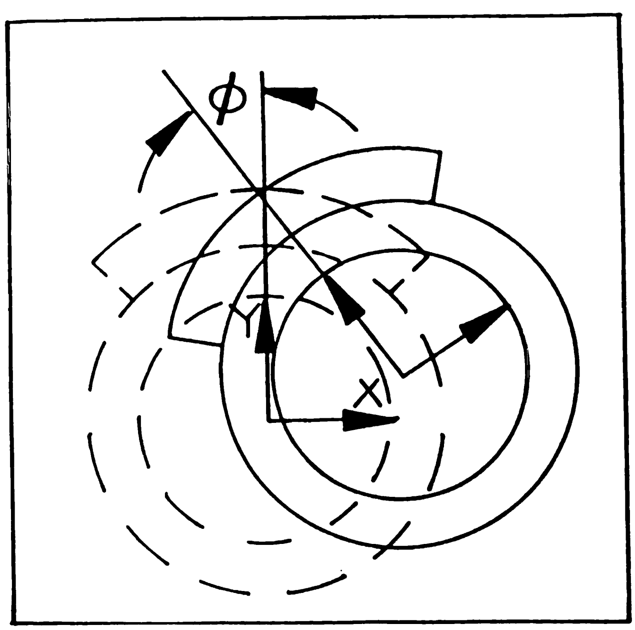

Figure 29. Out of Plane Rotation

Figure 30 shows the variation of this angle with plate stiffness for an upward bending load of 10 N-m.

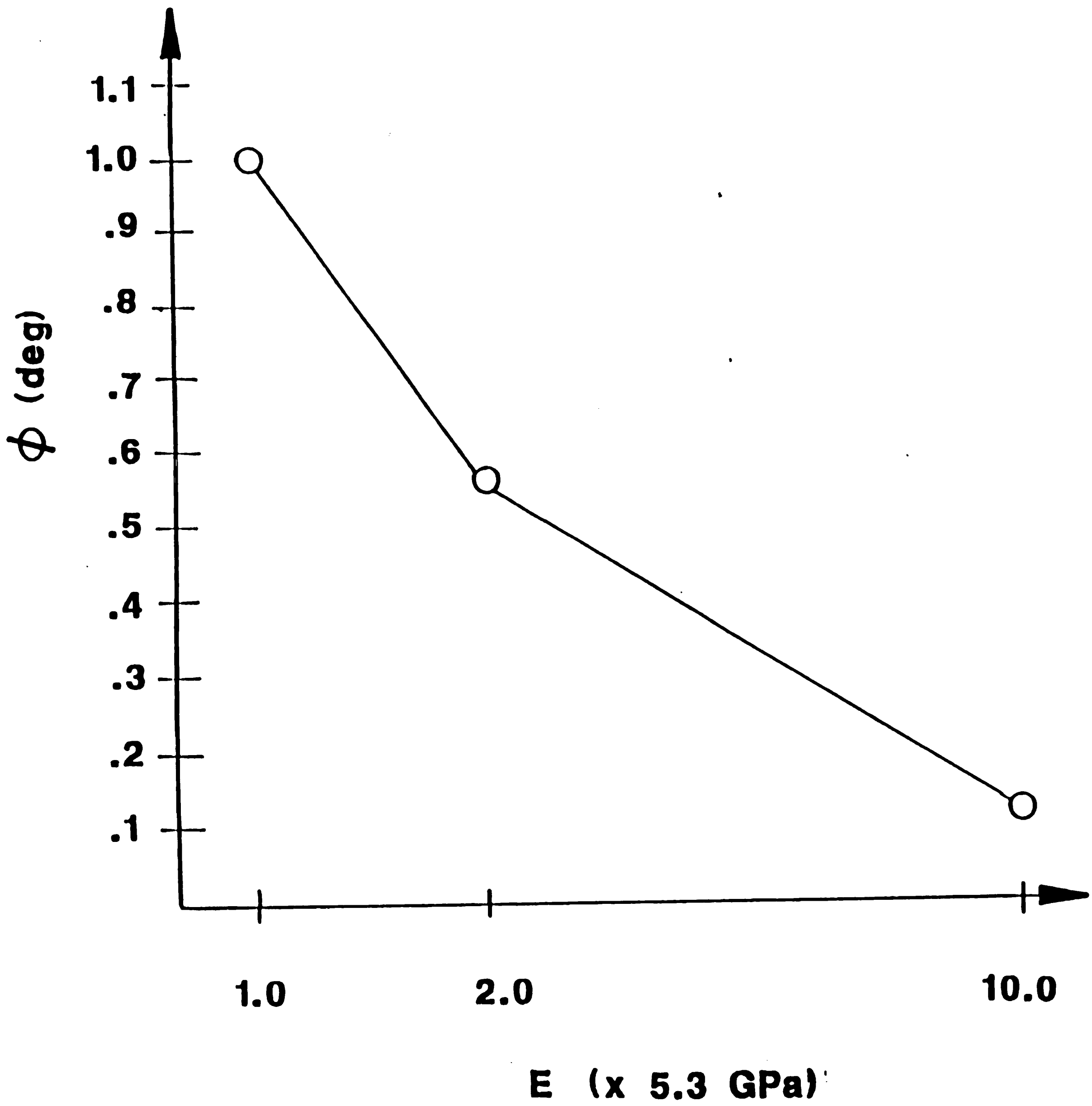

Figure 30. Rotation vs. Stiffness

For a plate modulus of 5.3×10^9 Pa, corresponding to a nylon like material, this angle is over 2^o. In the past, the materials used for plating were very stiff, steel or titanium for example. In this case, the out of plane rotation was insignificant, and therefore, attention was not paid to fastener pattern. With the mounting evidence on the detrimentel effects of these plates, a trend has developed to attempt to construct plates from more flexible materials such as plastic or nylon. The result of this is a dramatic increase in the magnitude of the out of plane rotation, and therefore, a dramatic increase in the possibility of type 4 failure.

VI. CONCLUSIONS

It was shown in chapter 3 that for loads of upward bending, the strength of materials model gave accurate in-plane displacements and fastener forces. This data could be used to evaluate the potential of fastener failure and non-union of the bone. It was later shown, however, that if plates with low bending stiffnesses were used, the out of plane rotation became a significant factor. In this case, the beam model failed to give an accurate assesment of failure potential.

The finite element model was shown, in chapter 4, to yield a converged solution for the stresses and three dimensional displacements in the system. Furthermore, in chapter 5, this data was shown to yield the necessary information for evaluation of all four potential failure modes in the form of: the stress field throughout the system for given loads and material properties, the normal and shear stresses in the fasteners and the in and out of plane displacements of the bone at the fracture sight.

The finite element model also exhibited a reversal in the load bearing role of the fasteners under a reversal in the applied load. One of the reasons this could be seen was the ability of the model to allow for stress free separation of the plate and bone. Recently, Beaupre et. al. (1988)[4] performed a finite element analysis in which the frictional nature of the plate bone interface was included. Their paper stated that failure to account for this effect may tend to overestimate the amount of stress shielding actually occuring.

Given a larger processor, a number of refinements would be made to the model presented in this paper. First, a frictional interface would be included for the reasons mentioned above. Next, a more realistic modelling of the fastener shapes and their boundary conditions would be included in order to more accurately assess the possibility of fastener failure due to bending and shear. Finally, the mesh density in the region surrounding the fasteners would be increased in order to obtain stress concentration values, thus facilitating a more realistic conclusion on the possibility of plate and bone failure due to excessive stresses.

Although some compromises were made in the models presented, they nevertheless have many merits which have been described above. Just as the strength of materials model acted as a starting point for the the finite element model, so then should this finite element model act as a foundation for further analyses, experimental or analytical, of the mechanics of plated bones.

APPENDIX

APPENDIX 1

The following calculations were used to adjust the moments of inertia for the plate and bone in the beam and finite element models.

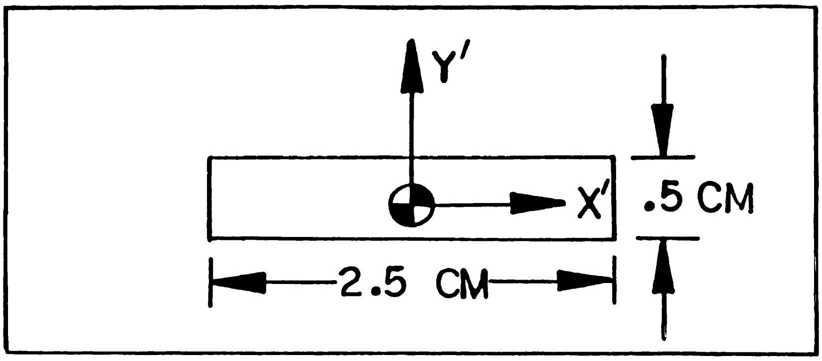

Figure 31. Cross Section i.

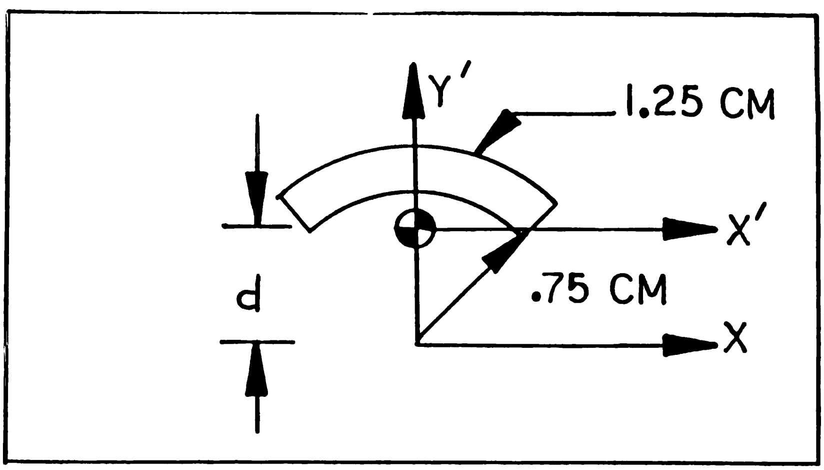

Figure 32. Cross Section ii.

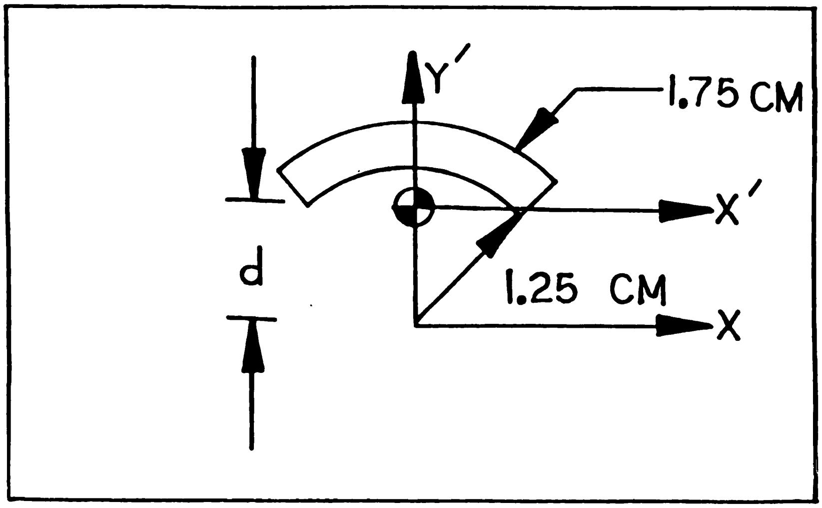

Figure 33. Cross Section iii.

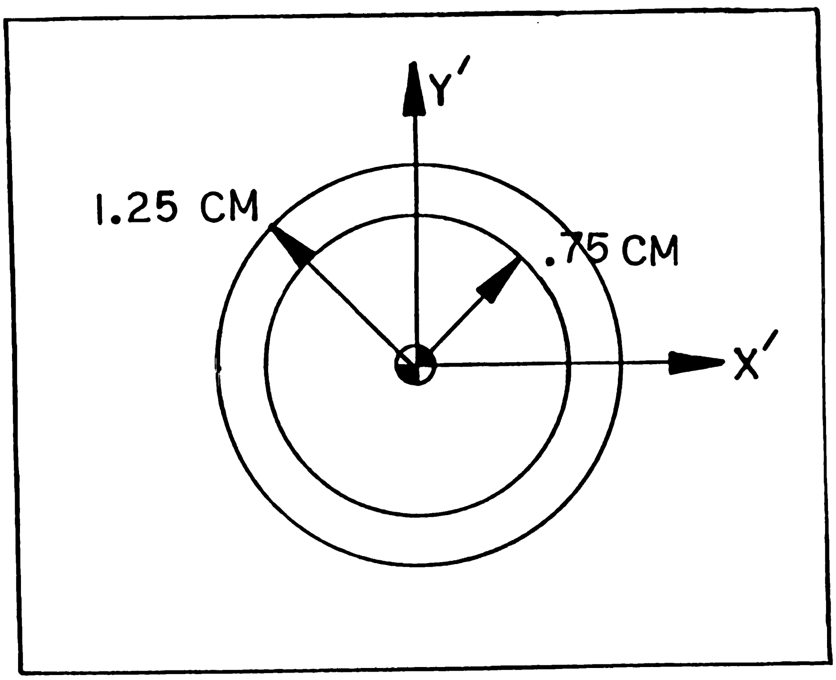

Figure 34. Cross Section iv.

Table 1. Cross sectional properties.

	i	ii	iii	iv
$A(mm^2)$	125.00	117.81	78.54	314.14
d(mm)	0.00	13.63	9.19	0.00
$I_{xx}(mm^4)$	260.417	22,239.6	6828.7	16,689.7
$I_{x'x'}$	260.47	354.5	194.7	16,689.7

The actual cross sections are:

1. Plate (ii)
2. Bone (iv)

When the plate or bone are represented by a shape other than their true cross section, their Youngs moduli are multiplied by the appropriate choice from the following list.

$I_p/I_i = 1.3614$, $I_b/I_i = 64.09$, $I_b/I_{iii} = 85.8$

Figure 35 demonstrates that these adjusted values yield valid bending responses. Displayed is the y-displacement, for an upward bending load, for all three cross sectional representations.

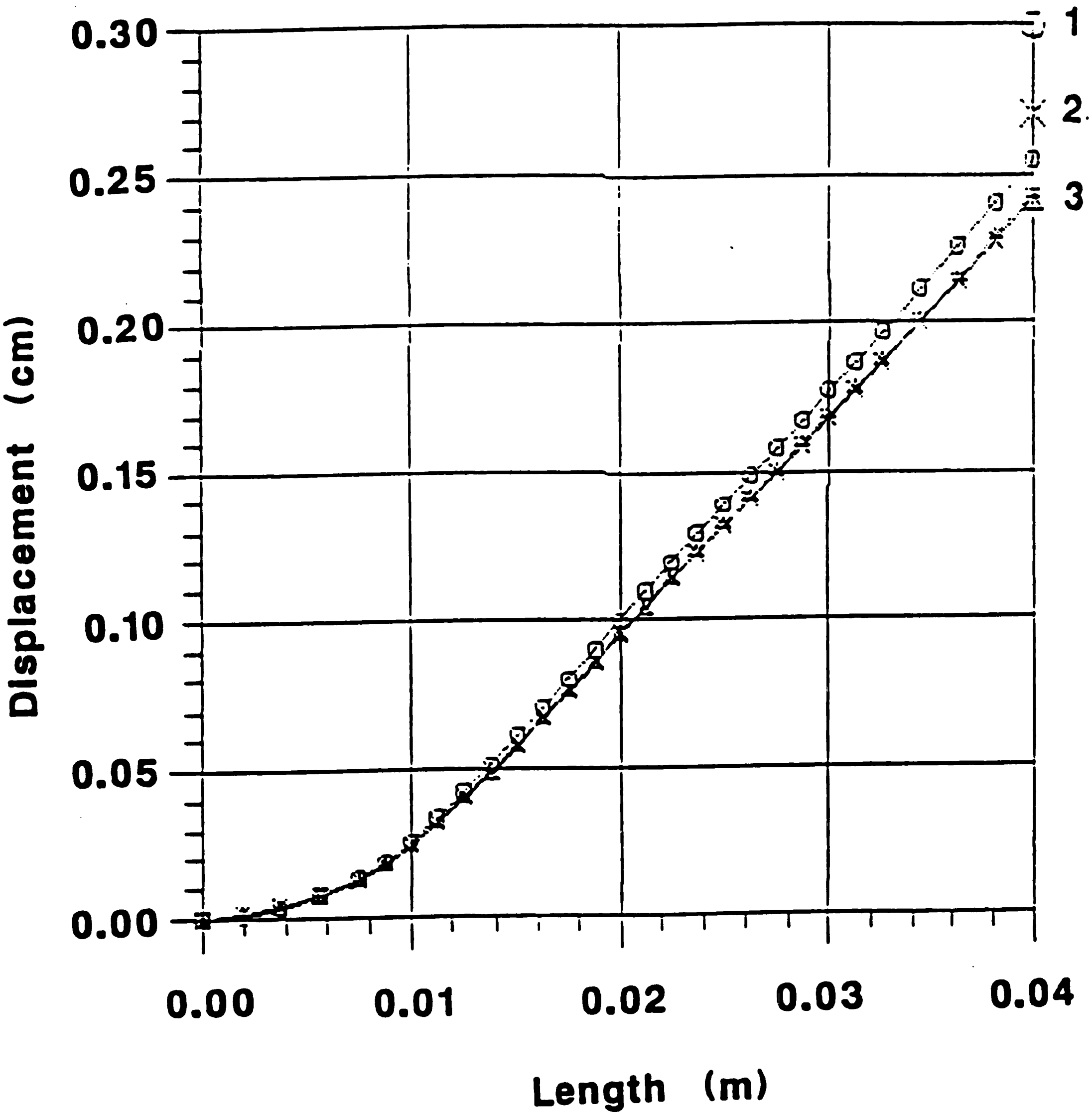

Figure 35. Cross Sectional Adjustment Results.

LIST OF REFERENCES

BIBLIOGRAPHY AND REFERENCES

1. Akeson, W.H., Woo, S., Coutts, R.D., Matthews, J.V., Gonsalves, M. and Amiel, D.: Quantitative histological evaluation of early fracture healing of cortical bones immobilized by stainless steel and composite plates. Calcif. Tissue Res., 19, 1975, pp. 27-37.

2. Askew, M.J., Mow, V.C. Wirth, C.R. and Campbell, C.J.: Analysis of the interosseous stress field due to compression plating. J. Biomechanics, 8, 1975, pp. 203-212.

3. Baggot, D.G., Goodship, A.E. and Lanyon, L.E.: A quantitative assesment of compression plate fixation in vivo:An experimental study using the sheep radius. J. Biomechanics, 14, 1981, pp. 701-711.

4. Beaupre, G.S., Carter, D.R., Orr, T.E. and Csongradi J.: Stresses in plated long bones: The role of screw tightness and interface slipping. J. Orthop. Res., 6, 1988, pp. 39-50.

5. Bynum, D.Jr., Allen, G.F., Ray, D.R. and Ledbetter, W.B.: In vitro performance of installed internal fixation plates in compression. J. Biomed. Mater. Res., 5, 1971, pp. 389-405.

6. Carter, D.R., Vasu, R., Spengler, D.M. and Dueland, R.T.: Stress fields in the unplated and plated canine femur calculated from in vivo strain measurements. J. Biomechanics, 14, 1981, pp. 63-70.

7. Carter, D.R. and Vasu, R.: Plate and bone stresses for single and double-plated femoral fractures. J. Biomechanics, 14, 1981, pp. 55-62.

8. Cheal, E.J., Hayes, W.C., White, A.A. III and Perren, S.M.: Three-dimensional finite element analysis of a simplified compression plate fixation system. J. Biomech. Eng., 106, 1984, pp. 295-301.

9. Cheal, E.J., Hayes, W.C., White, A.A. III and Perren, S.M.: Stress analysis of compression plate fixation and its effects on long bone remodeling. J. Biomechanics, 18, 1985, pp. 141-150.

10. Cochran, G.V.B.: Effects of internal fixation plates on mechanical deformation of bone. Surg. forum Orthorpaed. Surg., 20, 1969, pp. 469-471.

11. Godfrey, L.J.: Looking at bone plates and screws. Eng. in Med., 1, 1971, pp. 17-18.

12. Goodship, A.E., Lanyon, L.E. and McFie, H.: Functional adaptation of bone to increased stress. J. Bone and Joint Surg., 61-A, 1979, pp. 539-546.

13. Horwitz, T. and Lambert, R.G.: Treatment of ununited fractures of long bones: A method combining grafting and internal fixation. J. Bone and Joint Surg., 27, 1945, pp. 637-644.

14. Key, J.A.: Dual plates for internal fixation in non-union of fractures. J. Bone and Joint Surg., 27, 1945, pp. 632-636.

15. Koch, J.C.: The laws of bone architecture. Am. J. Anat., 21, 1917, 177-298

16. Lanyon, L.E. and Baggott, D.G.: Mechanical function as an influence on the structure and form of bone. J. Bone and Joint Surg., 58-B, 1976, pp. 436-443.

17. Laurence, M., Freeman, M.A.R. and Swanson, S.A.V.: Engineering considerations in the internal fixation of fractures of the tibial shaft. J. Bone and Joint Surg., 51-B, 1969, pp.754-768.

18. Melkerson, M.: Experimental results obtained in 1987

19. Murray, C.R.: Primary operative fixation in fractures of the long bones in adults. Am. J. Surg., LI, 1941, pp. 739-747.

20. Perren, S.M., Russenberger, M., Steinemann, S. et al.: A dynamic compression plate. Acta. Orthop. Scand., 1969, 125.

21. Rahn, B.A., Gallinaro, P, Baltensperger, A. and Perren, S.M.: Primary bone healing. J. Bone and Joint Surg., 53-A, 1971, pp. 783-786.

22. Ray, D.R., Ledbetter, W.B., Bynum, D. and Boyd, C.L.: A parametric analysis of bone fixation plates on fractured equine third metacarpal. J. Biomechanics, 4, 1971, pp. 163-174.

23. Reddy, J.N.: An introdution to the finite elemet method, McGraw-Hill Book Company, N.Y., 1984, pp. 235-238.

24. Rybicki, E.F. and Simonen, F.A.: Mechanics of oblique fracture fixation using a finite-element model. J. Biomechanics, 10, 1977, pp. 141-148.

25. Rybicki, E.F., Simonen, F.A. and Weis, E.B. Jr.: On the mathematical analysis of stress in the human femur. J. Biomechanics, 5, 1972, pp. 203-215.

26. Rybicki, E.F., Simonen, F.A., Mills, E.J., Hassler, C.R., Scoles, P., Milne, D. and Weis, E.B.: Mathematical and experimental studies on the mechanics of plated transverse fractures. J. Biomechanics, 7, 1974, pp. 377-384.

27. Simon, B.R., Woo, S., Stanley, G.M., Olmstead, S.R., McCarty, M.P., Jemmott, G.F. and Akeson, W.H.: Evaluation of one-, two-, and three-dimensional finite element and experimental models of internal fixation plates. J. Biomechanics, 10, 1977, pp. 78-86.

28. Slatis, P., Karaharju, E., Holmstrom, T., Ahonen, J. and Paavolainen, P.: Structural changes in intact tubular bone after application of rigid plates with and without compression. J. Bone and Joint Surg., 60-A, 1978, pp. 516-522.

29. Terjesen, T., Apalset, K.: The influence of different degrees of stiffness of fixation plates on experimental bone healing. J. Orthop. Res., 6, 1988, 293-299.

30. Tonino, A.J., Davidson, C.L., Klopper, P.J. and Linclau, L.A.: Protection from stress in bone and its effects: Experiments with stainless steel and plastic plates in dogs. J. Bone and Joint Surg., 58-B, 1976, pp. 107-113.

31. Uhtoff, H.K. and Dubuc, F.L.: Bone structure changes in the dog under rigid internal fixation. Clin. Orthop. and Rel. Res., 81, 1971, pp. 165-170.

32. Uhtoff, H.K. and Jaworski, Z.F.G.: Bone loss in response to long-term immobilisation. J. Bone and Joint Surg., 60-B, 1978, pp. 420-429.

33. Van Buskirk, W.C. and Ashman, R.B.: The elastic moduli of bone. Mechanical Properties of Bone, The joint ASME-ASCE Applied Mechanics, Fluids Engineering and Bioengineering Conference, 1981, pp. 131-143.

34. Wienberger, H.F.: A first course in partial diffential equations, John Wiley and Sons, Inc., N.Y., 1965, pp. 81-87.

35. Wilson, E.L., Taylor, R.L., Doherty, W.P.: Incompatible displacement models. Numerical and Computer Methods in Structural Mechanics., Ed. S.J. Fenves et. al., Academic Press, N.Y., 1973, pp. 43-57.

36. Wolff, J.: Das gesetz der transformation der knochen. Quarto. Berlin.

37. Woo, S., Akeson, W.H., Coutts, R.D., Rutherford, L., Doty, D., Jemmott, G.F. and Amiel, D.: A comparison of cortical bone atrophy secondary to fixation with plates with large differences in bending stiffness. J. Bone and Joint Surg., 58-A, 1976, pp. 190-195.

38. Woo, S., Simon, B.R., Akeson, W.H. and McCarty, M.P.: An interdisciplinary approach to evaluate the effect of internal fixation plate on long bone remodeling. J. Biomechanics, 10, 1977, 87-95.